

DOE/BC/14986-3
(DE95000142)

CO₂ HUFF-n-PUFF PROCESS IN A LIGHT OIL
SHALLOW SHELF CARBONATE RESERVOIR

1994 Annual Report

By
Scott Wehner

May 1995

Performed Under Contract No. DE-FC22-94BC14986

Texaco Exploration & Production Inc.
Midland, Texas

**FOSSIL
FUELS
AGENCY**



**Bartlesville Project Office
U. S. DEPARTMENT OF ENERGY
Bartlesville, Oklahoma**

DISCLAIMER

This report was prepared as an account of work sponsored by an agency of the United States Government. Neither the United States Government nor any agency thereof, nor any of their employees, makes any warranty, expressed or implied, or assumes any legal liability or responsibility for the accuracy, completeness, or usefulness of any information, apparatus, product, or process disclosed, or represents that its use would not infringe privately owned rights. Reference herein to any specific commercial product, process, or service by trade name, trademark, manufacturer, or otherwise does not necessarily constitute or imply its endorsement, recommendation, or favoring by the United States Government or any agency thereof. The views and opinions of authors expressed herein do not necessarily state or reflect those of the United States Government or any agency thereof.

This report has been reproduced directly from the best available copy.

Available to DOE and DOE contractors from the Office of Scientific and Technical Information, P.O. Box 62, Oak Ridge, TN 37831; prices available from (615) 576-8401.

Available to the public from the National Technical Information Service, U.S. Department of Commerce, 5285 Port Royal Rd., Springfield VA 22161

DOE/BC/14986-3
Distribution Category UC-122

**CO₂ HUFF-n-PUFF PROCESS IN A LIGHT OIL
SHALLOW SHELF CARBONATE RESERVOIR**

1994 Annual Report

**By
Scott C. Wehner**

May 1995

Work Performed Under Contract No. DE-FC22-94BC14986

**Prepared for
U.S. Department of Energy
Assistant Secretary for Fossil Energy**

**Jerry Casteel, Project Manager
Bartlesville Project Office
P.O. Box 1398
Bartlesville, OK 74005**

**Prepared by
Texaco Exploration & Production Inc.
500 North Loraine
Midland, TX 79701**

Table of Contents

List of Figures	v
List of Tables	vii
Abstract	1
Executive Summary.....	2
Introduction:	
Field History.....	4
Geology.....	4
Brief of Project & Technology Description	6
Discussion:	
Macro Zonation & Cross Sections	8
Initial Water Saturation Distribution & OWC.....	10
Net Pay Determination.....	15
Permeability Relationships	16
Geostatistical Realizations	19
Waterflood Review.....	20
Development of an Equation-of-State	21
Parametric Simulations	31
References and Appendices	33

LIST OF FIGURES

1	Unitized Acreage of Vacuum Field	1
2	Permian Basin and Relative Position of Vacuum Field.....	2
3	Visual Illustration of CO ₂ Huff-n-Puff Process.....	3
4	Index Map of Available Cross Sections.....	4
5	Example Cross Section.....	5
6	Capillary Pressure vs S _w , VGSAU Well No. 140.....	6
7	Wireline Derived S _w vs Capillary Pressure Derived Data, VGSAU No. 140.....	7
8	Leverett “J” Function S _w Profile vs E-log profile, VGSAU No. 140.....	8
9	Neural Network Permeability Solution Relative to Test Set	9
10	Flow Diagram of Neural Network Permeability Assignments	10
11	Comparison Of Laboratory Data and EOS Prediction of Liquid Volume Fraction as a Function of Pressure for No Added CO ₂	11
12	Comparison of Laboratory Data and EOS Prediction of Relative Volume as a Function of Pressure for No Added CO ₂	12
13	Comparison of Laboratory Data and EOS Prediction of Liquid Volume Fraction as a Function of Pressure for 20 Mole-% Added CO ₂	13
14	Comparison of Laboratory Data and EOS Prediction of Relative Volume as a Function of Pressure for 20 Mole-% Added CO ₂	14
15	Comparison of Laboratory Data and EOS Prediction of Liquid Volume Fraction as a Function of Pressure for 41 Mole-% Added CO ₂	15
16	Comparison of Laboratory Data and EOS Prediction of Relative Volume as a Function of Pressure for 41 Mole-% Added CO ₂	16
17	Comparison of Laboratory Data and EOS Prediction of Liquid Volume Fraction as a Function of Pressure for 55 Mole-% Added CO ₂	17

18	Comparison of Laboratory Data and EOS Prediction of Relative Volume as a Function of Pressure for 55 Mole-% Added CO ₂	18
19	Comparison of Laboratory Data and EOS Prediction of Liquid Volume Fraction as a Function of Pressure for 70 Mole-% Added CO ₂	19
20	Comparison of Laboratory Data and EOS Prediction of Liquid Volume Fraction as a Function of Pressure for 75 Mole-% Added CO ₂	20
21	Comparison of Laboratory Data and EOS Prediction of Liquid Volume Fraction as a Function of Pressure for 85 Mole-% Added CO ₂	21
22	Comparison of Laboratory Data and EOS Prediction of Liquid Viscosity as a Function of Pressure for No Added CO ₂	22
23	Comparison of Laboratory Data and EOS Prediction of Liquid Viscosity as a Function of Pressure for 41 Mole-% Added CO ₂	23
24	Comparison of Laboratory Data and EOS Prediction of Liquid Viscosity as a Function of Pressure for 55 Mole-% Added CO ₂	24
25	Comparison of Established Data and EOS Prediction of Pure CO ₂ Density as a Function of Pressure.....	25
26	Comparison of Laboratory Slimtube Data and EOS Prediction Of Oil Recovery as a Function of Injected CO ₂ Volume for Selected Pressures.....	26

LIST OF TABLES

1	Results of Porosity & Permeability Cutoff Study.....	1
2	Pseudocomponenet System for Compositional Simulation.....	2
3	CO ₂ - Oil Mixture Saturation Pressures.....	3

ABSTRACT

Texaco E & P Inc. and the U. S. Department of Energy have teamed up in an attempt to develop the CO₂ Huff-n-Puff process in a light oil, shallow shelf carbonate reservoir within the Permian Basin. This cost-shared effort is intended to demonstrate the viability of this underutilized technology in a specific class of domestic reservoirs that are considered to be at risk of abandonment^{1,2}. The selected site for the demonstration project is the Central Vacuum Unit waterflood in Lea County, New Mexico.

The CO₂ Huff-n-Puff process is a proven enhanced oil recovery technology in Louisiana-Texas gulf coast sandstone reservoirs^{3,4}. Application seems to mostly confine itself to low pressure sandstone reservoirs⁵. The process has even been shown to be moderately effective in conjunction with steam on heavy California crude oils^{6,7}. A review of earlier literature^{3,8,9} provides an excellent discussion on the theory, mechanics of the process, and several case histories. Although the technology is proven in light oil sandstones, it continues to be a very underutilized enhanced recovery option for carbonates.

It is anticipated that this project will show that the application of the CO₂ Huff-n-Puff process in shallow shelf carbonates can be economically implemented to recover appreciable volumes of light oil. The goals of the project are the development of guidelines for cost-effective selection of candidate reservoirs and wells, along with estimating recovery potential.

This project has two defined budget periods. The first budget period primarily involves tasks associated with reservoir analysis and characterization, characterizing existing producibility problems, and reservoir simulation of the proposed technology. The final budget period will cover the actual field demonstration of the proposed technology. Technology transfer spans the entire course of the project. It is the first budget period that is partially covered in this report.

Work is nearing completion on the reservoir characterization components of the project. The near-term emphasis is to, 1) provide an accurate distribution of original oil-in-place on a waterflood pattern entity level, 2) evaluate past recovery efficiencies, 3) perform parametric simulations, and 4) forecast performance for a site specific field demonstration of the proposed technology. Macro zonation now exists throughout the study area and cross-sections are available. The Oil-Water Contact has been defined. Laboratory capillary pressure data was used to define the initial water saturations within the pay horizon. The reservoir's porosity distribution has been enhanced with the assistance of geostatistical software. Three-Dimensional kriging created the spacial distributions of porosity at inter-well locations. Artificial intelligence software was utilized to relate core permeability to core porosity, which in turn was applied to the 3-D geostatistical porosity gridding. An Equation-of-State has been developed and refined for upcoming compositional simulation exercises. Options for local grid-refinement in the model are under consideration. These tasks will be completed by mid-1995, prior to initiating the field demonstrations in the second budget period.

A successful demonstration of the CO₂ Huff-n-Puff process could have wide application. The proposed technology promises several advantages. It is hoped that the CO₂ Huff-n-Puff process might bridge near-term needs of maintaining the large domestic resource base of the Permian Basin until the mid-term economic conditions support the implementation of more efficient, and prolific, full-scale miscible CO₂ projects.

EXECUTIVE SUMMARY

Texaco Exploration and Production Inc. (TEPI) was awarded a contract from the Department of Energy (DOE) during the first quarter of 1994. This contract is in the form of a cost-sharing Cooperative Agreement (Project). The goal of this joint Project is to demonstrate the Carbon Dioxide (CO₂) Huff-n-Puff (H-n-P) process in a light oil, shallow shelf carbonate (SSC) reservoir within the Permian Basin. The selected site is the TEPI operated Central Vacuum Unit (CVU) waterflood in Lea County, New Mexico.

TEPI's long-term plans are to implement a full-scale miscible CO₂ project in the CVU. However, the current market precludes acceleration of such a capital intensive project. This is a common finding throughout the Permian Basin SSC reservoirs. In theory, it is believed that the "immiscible" CO₂ H-n-P process might bridge this longer-term "miscible" project with near-term results. A successful implementation would result in near-term production, or revenue, to help offset cash outlays of the capital intensive miscible CO₂ project. The DOE partnership provides some relief to the associated R & D risks, allowing TEPI to evaluate a proven Gulf-coast sandstone technology in a waterflooded carbonate environment. A successful demonstration of the proposed technology would likely be replicated within industry many fold--resulting in additional domestic reserves.

The principal objective of the CVU CO₂ H-n-P project is to determine the feasibility and practicality of the technology in a waterflooded SSC environment. The results of parametric simulation of the CO₂ H-n-P process coupled with reservoir characterization will assist in determining if this process is technically and economically ready for field implementation. The ultimate goal will be to develop guidelines based on commonly available data that operators within the oil industry can use to investigate the applicability of the process within other fields. The technology transfer objective of the project is to disseminate the knowledge gained through an innovative plan in support of the DOE's objective of increasing domestic oil production and deferring the abandonment of SSC reservoirs. Tasks associated with this objective are carried out in what is considered a timely effort.

The application of CO₂ technologies in Permian Basin carbonates may do for the decade of the 1990's and beyond, what waterflooding did for this region beginning in the 1950's. With an infrastructure for CO₂ deliveries already in place, a successful demonstration of the CO₂ H-n-P process could have wide application. The proposed technology promises a number of economical advantages. Profitability of marginal properties could be maintained until such time as pricing justifies a full-scale CO₂ miscible project. It could maximize recoveries from smaller isolated leases which could never economically support a miscible CO₂ project. The process, when applied during the installation of a full-scale CO₂ miscible project could mitigate up-front negative cash-flows, possibly to the point of allowing a project to be self-funding and increase horizontal sweep efficiency at the same time. Since most full-scale CO₂ miscible projects are focused on the "sweet spots" of a property, the CO₂ H-n-P process could concurrently maximize recoveries from non-targeted acreage. An added incentive for the early application of the CO₂ H-n-P process is that it could provide an early measure of CO₂ injectivity of future full-scale CO₂ miscible projects and improve real-time recovery estimates--reducing economic risk. It is hoped that the CO₂ H-n-P process might bridge near-term needs of maintaining the large

domestic resource base of the Permian Basin until the mid-term economic conditions support the implementation of more efficient, and prolific, full-scale miscible CO₂ projects.

This project has two defined budget periods. The first budget period primarily involves tasks associated with reservoir analysis and characterization, characterizing existing producibility problems, and reservoir simulation of the proposed technology. The final budget period will cover the actual field demonstration of the proposed technology. Technology transfer spans the entire course of the project. It is the first budget period that is partially covered in this report.

Work is nearing completion on the reservoir characterization components of the project. The near-term emphasis is to, 1) provide an accurate distribution of original oil-in-place on a waterflood pattern entity level, 2) evaluate past recovery efficiencies, 3) perform parametric simulations, and 4) forecast performance for a site specific field demonstration of the proposed technology. Macro zonation now exists throughout the study area and cross-sections are available. The Oil-Water Contact has been defined. Laboratory capillary pressure data was used to define the initial water saturations within the pay horizon. The reservoir's porosity distribution has been enhanced with the assistance of geostatistical software. Three-Dimensional kriging created the spacial distributions of porosity at inter-well locations. Artificial intelligence software was utilized to relate core permeability to core porosity, which in turn was applied to the 3-D geostatistical porosity gridding. An Equation-of-State has been developed and refined for upcoming compositional simulation exercises. Options for local grid-refinement in the model are under consideration. These tasks will be completed by mid-1995, prior to initiating the field demonstrations in the second budget period.

INTRODUCTION

FIELD HISTORY

The Vacuum Field was discovered in May, 1929 by the Socony Vacuum Oil Company--now known as Mobil. The discovery well was the New Mexico "Bridges" State Well No. 1 (drilled on the section line of Sec's 13 & 14, T16S R34E). The well was shut-in until 1937 when pipeline facilities became available to the area. Field development began in late 1937 and by 1941, 327 wells had been completed on 40-acre spacings. By year 1947, the field had been extended approximately two miles to the west. Scattered reservoir development continued slowly over the next two decades. The CVU became official in 1977 with water injection beginning in 1978. The CVU was infill drilled on 20-acre spacings during the period 1978-1982. A polymer augmented waterflood was incorporated and completed during the 1980's. Further reservoir development began in the late 1980's with sporadic infill drilling on 10-acre spacings. Sporadic infill development continues. Enhanced recovery operations by waterflooding are in progress across the entire Vacuum field, and CO₂ Miscible Flooding was initiated by Phillips in the southeastern portion of the field, immediately east of the CVU. Figure 1 identifies the Unitized operations of the Vacuum field. In addition to the San Andres/Grayburg producing horizons, there are 12 other formations that are, or have been productive in the Vacuum field. These, mostly deeper horizons were developed predominantly during the 1960's.

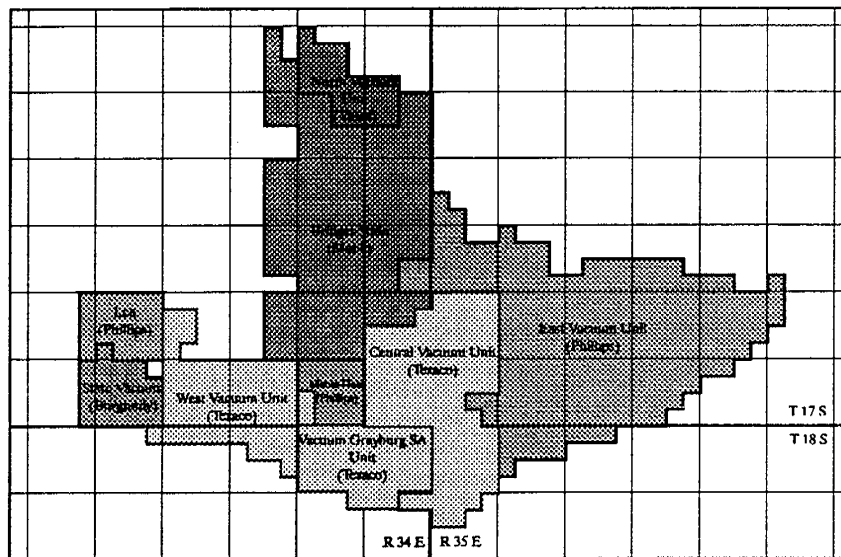


Figure 1: Unitized Acreage of Vacuum Field, Lea Co., New Mexico.

GEOLOGY

The CVU is located 22 miles west of Hobbs, New Mexico in Lea County. The Vacuum field lies on the southern edge of the Northwest Shelf (or northern limit of the Delaware Basin) along a productive east-west-trending shelf area of the Permian Basin--known locally as the Artesia-Vacuum trend. Figure 2 identifies the position of the Vacuum field in the Permian Basin. Production in these Units is primarily from the Permian Guadalupian age San Andres formation with a lesser amount from the

overlying Grayburg formation. The productive interval parallels an ancient shelf to basin depositional trend south and southeast of Vacuum field. The San Andres is composed of cyclical evaporites and carbonates recording the many "rises" (transgressing) and "falls" (regressing) of sea level occurring around 260 million years ago in a climate very similar to the present day Persian Gulf. The San Andres pay zone is divided by the Lovington sand member. The Grayburg formation is composed of cyclical carbonates and sands. The oil has been trapped in porous dolomites and sands that developed on a structural high. The productive intervals are sealed by overlying evaporites. Stratigraphically to the north, the porous dolomites pinch out into non-porous evaporites and evaporite filled dolomites. The porous zones dip below the oil water contact in the southerly/basinward direction.

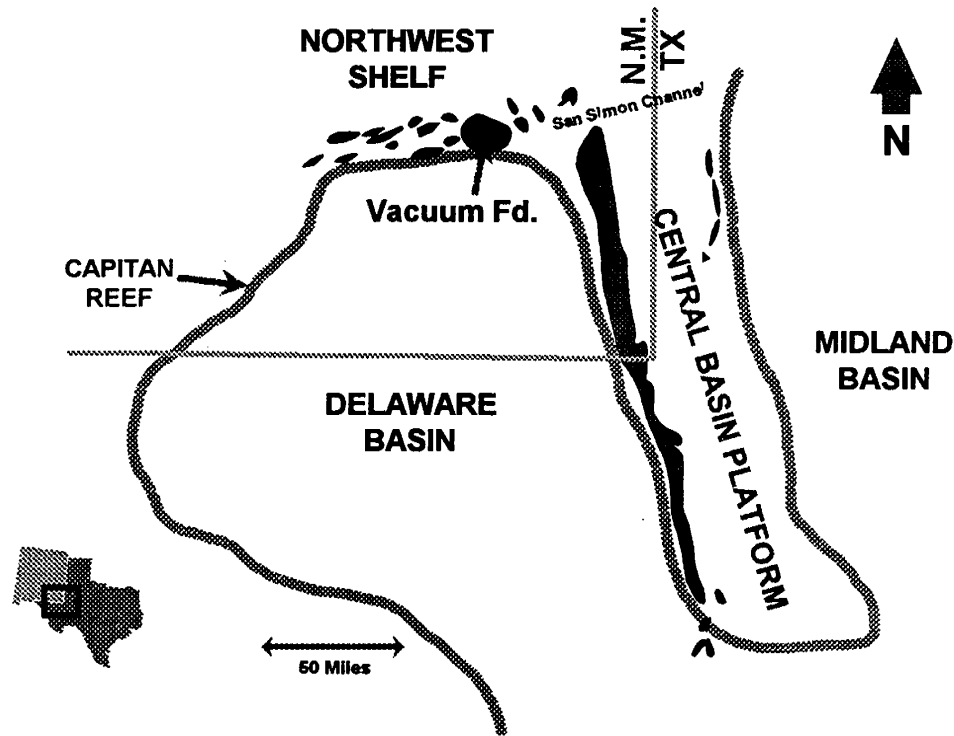


Figure 2: Permian Basin and relative position of Vacuum field.

Lithologically, the Grayburg formation consists of dense gray dolomite with some anhydrite. It contains interbedded dolomitic sand stringers. Log and core data indicate that this formation has a very small reserve contribution relative to the San Andres formation. The San Andres formation consists of dense medium crystalline and oolitic dolomite, white to gray in color, with some anhydrite. The pay is a fine to medium crystalline oolitic dolomite with slight fracturing and some solution cavities. Productive intervals consist of a series of permeable beds separated by impermeable strata. The strata extend over large areas of the field and are believed to serve as effective barriers to prevent cross-flow between the permeable beds.

The Grayburg/San Andres formations produce a 38.0° API oil from an average depth of 4550' within the CVU. The original water-free oil column reached as much as 600'. Porosity and permeability in the gross pay interval can reach a maximum of 23.7%, and 530 md, respectively. The porosity and permeability over the gross pay interval averages 6.8% and 9.7 md, respectively. Based on core

studies, the net productive pay averages 11.6 % porosity and 22.3 md. Although the residual oil saturation to waterflooding within the near wellbore vicinity has not yet been determined in detail, carbonate reservoirs typically leave behind a high residual oil saturation in the range of 30-35% in the waterflood swept zones. Oil saturations in unswept zones, created by the heterogeneous nature of the reservoir approach initial conditions. This is a significant volume of uncontacted and immobile oil which is the target of this CO₂ H-n-P process.

BRIEF of PROJECT & TECHNOLOGY DESCRIPTION

This project has two defined budget periods. This report covers work performed to-date under the first budget period. The first budget period primarily involves tasks associated with reservoir analysis and characterization, characterizing existing producibility problems, and reservoir simulation of the proposed technology. The near-term emphasis is to, 1) provide an accurate distribution of original oil-in-place on a waterflood pattern entity level, 2) evaluate past recovery efficiencies, 3) perform parametric simulations, and 4) forecast performance for a site specific field demonstration of the proposed technology. The second, and final budget period incorporates the actual field demonstration of the technology.

Reservoir characterization and a thorough waterflood review will help identify sites for performance of the field demonstrations. Numerical simulation will help define the specific volumes of CO₂ required, best operational practices, and expected oil recoveries from the demonstration sites. The typical process cycle will involve the injection of an estimated 500 tons CO₂ in a producing well. The CO₂ will be injected in an immiscible condition, displacing the majority of the mobile water within the wellbore vicinity, while bypassing the oil-in-place. The CO₂ will be absorbed into both the oil and remaining water. The water will absorb CO₂ quickly, but only a relatively limited quantity. Conversely, the oil can absorb a significant volume of CO₂, although it is a much slower process. For this reason the producing well will be shut-in for what is termed a soak period. This soak period is expected to last 1-4 weeks depending upon fluid and reservoir properties. The pressure in the near-wellbore vicinity will continue to increase to near minimum miscibility conditions during the soak due to the active waterflood. During this soak period the oil will experience significant swelling, viscosity and interfacial tensions will be reduced, and the relative mobility of the oil will increase. The no-flow pressure boundary of the waterflood pattern will serve to confine the CO₂, reducing leak-off concerns. When the well is returned to production the mobilized oil will be swept to the wellbore by the waterflood. Incremental production is expected to return to its base level within 6 months. Previous work has shown that diminishing returns are expected with each successive cycle, thus this proposal is to expose each of the producers to no more than three cycles of the CO₂ H-n-P process over a two year period. Figure 3 visually illustrates the proposed CO₂ H-n-P process.

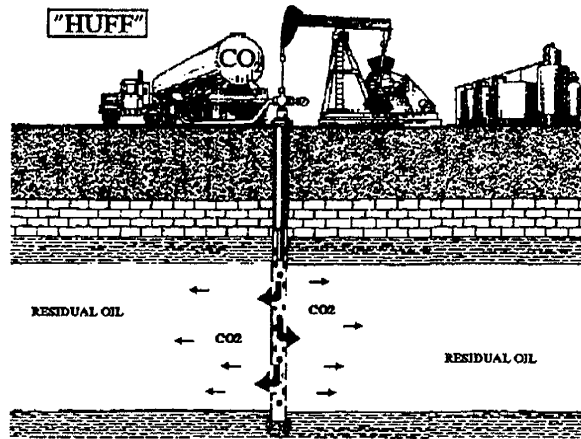


Figure 3a: Injection, or "Huff" phase of Project.

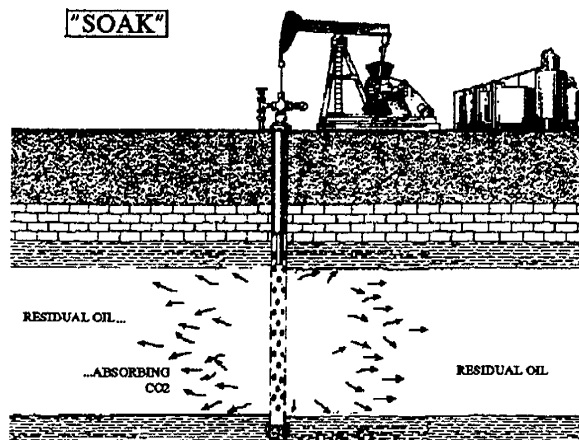


Figure 3b: The "Soak" phase of the Project.

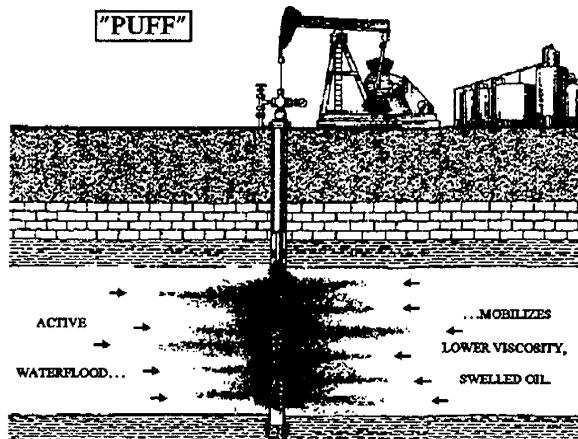


Figure 3c: The production, or "Puff" phase of the Project.

DISCUSSION

Work is nearing completion on the reservoir characterization components of the project. Macro zonation exists throughout the study area and cross-sections are now available. The Oil-Water Contact has been defined. Laboratory capillary pressure data was used to define the initial water saturations within the pay horizon. The reservoir's porosity distribution has been enhanced with the assistance of geostatistical software. Three-Dimensional kriging created the spacial distributions of porosity at inter-well locations. Artificial intelligence software was utilized to relate core permeability to core porosity, which in turn was applied to the 3-D geostatistical porosity gridding. An Equation-of-State has been developed and refined for upcoming compositional simulation exercises. Options for local grid-refinement in the model are under consideration. These tasks will be completed by mid-1995, prior to initiating the field demonstrations in the second budget period.

MACRO ZONATION & CROSS SECTIONS

A total of 455 wellbores penetrate the Grayburg and San Andres formation within the project study area. Cross sections through all wells within the subject producing horizons on Texaco operated acreage within the project study area were completed. An index map of the cross sections is provided in Figure 4. These cross sections were stratigraphically hung on the Grayburg Marker. Formation tops shown on the cross sections include (where identified/present) the Grayburg Dolomite, Grayburg Sandstone (non-pay), San Andres Sandstone (non-pay), Upper San Andres, Lovington Sandstone (non-pay), and the Lower San Andres. These tops represent the macro zonation based on a deterministic approach. The cross sections were developed using the commercial software, GeoGraphix Evaluation System. An example cross-section is shown in Figure 5. Completion histories will be included on the cross-sections. The cross sections assist in the understanding of the reservoir architecture, providing a quick review of correlative zones while reviewing waterflood histories.

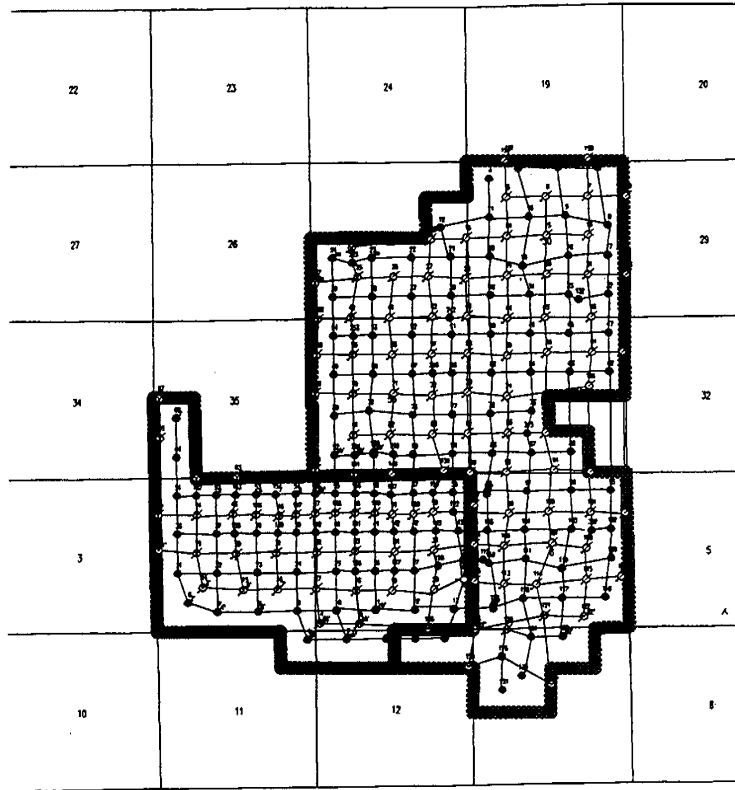


Figure 4: Index map of available cross sections.

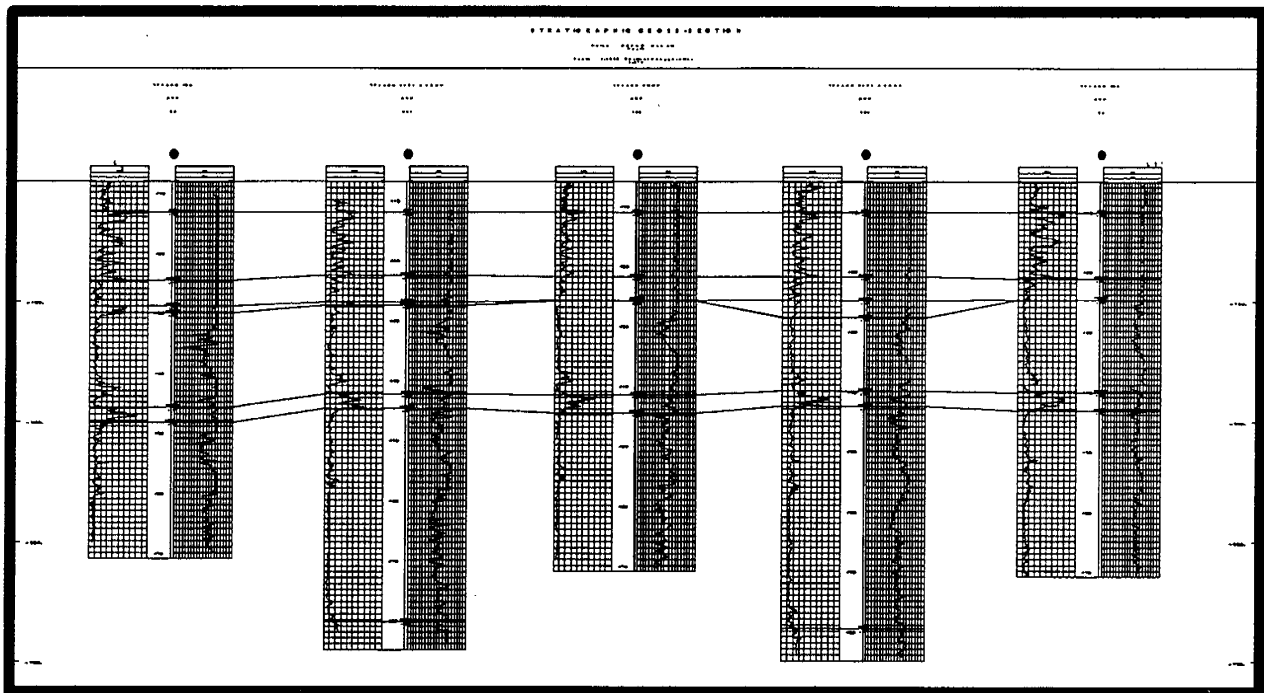


Figure 5: Example cross section within project study area.

INITIAL WATER SATURATION DISTRIBUTION & OWC

One of the major milestones associated with the reservoir characterization component of the project is determination of Original Oil-in-Place (OOIP). Therefore, an evaluation of fluid saturation was warranted. Initial water saturation (S_{wi}) distribution in a given reservoir is a function of capillary pressure¹⁰⁻¹². Laboratory derived capillary pressure data, corrected for reservoir conditions, can be used to define initial saturations above an Oil-Water Contact (OWC), or zero capillary pressure level ($S_w=100\%$). This study defined the OWC to be at -1,000' from sea level datum. The average S_{wi} of the main pay zone was established at 20.0 % using the wireline log and capillary pressure data.

It was first necessary to establish the OWC in order to apply the capillary pressure data. Historically, operators within the field have used various "OWC's" ranging from -700' to -775' from sea level¹³⁻¹⁷. This datum was probably established by drillers during the early development of the field as the deepest point for a water-free completion. This depth however is not the OWC, but is an average representation of the end point on the relative permeability curve corresponding to the irreducible water saturation, S_{wir} . This depth will be referred to as the top of a transition zone (TZ). A review of original depths for wells within the CVU & VGSAU found the average well depth to be at -700' from sea level. Very few wells had produced any measurable water above this depth by 1945¹³ and few would make any water prior to waterflooding operations in the 1970's. The majority of water encountered above the TZ in current operations has therefore been introduced by waterflooding operations. All known/documented tests within the TZ were included in this OWC study.

The task of establishing the true OWC, or bottom of the TZ, was accomplished by standard electric wireline log (E-log) evaluation techniques. Until recently, the unavailability of useable E-logs prohibited an accurate estimate of the OWC. Most of the E-logs that previously existed did not penetrate the TZ. Up until 1990, only 26 of the existing 85 E-logs penetrated enough of the formation to evaluate any part of the TZ, and only five of these were logged prior to waterflood influence. The few E-logs that did penetrate the TZ were found to be of questionable quality due to their vintage. Deeper drilling locations also yielded a few useable E-logs. Since 1990, an additional 68 E-logs (penetrating the TZ) have been obtained within, or in near proximity to, the CVU & VGSAU boundaries. A 10-acre infill drilling program within the San Andres formation, beginning in 1990, provided an additional 23 E-logs. A large-scale infill drilling program to the deeper Glorieta formation, beginning in 1991 provided an opportunity to gather another 45 E-logs across the TZ of the San Andres formation. As expected, the waterflood influence on these more recent logs caused a distortion of the shallower data, making log analysis difficult. However, in spite of the alteration from initial conditions in some zones, many of these new logs were found to be adequate due in part to compartmentalization and discontinuities within the reservoir. A "ghost" or "shadow" of the original saturation profile can be identified due to these heterogeneities. Some 10-Acre infill locations even exhibited a classic, uninfluenced saturation profile.

A thorough study of all available data suggests that the OWC be defined at approximately -1,000' from sea level datum. A review of the geological structure within the region containing the Vacuum field suggests that there is field closure to the north, east and south at approximately -800' from sea level. Hydrodynamic forces should be acting from the updip, northwesterly direction. However, the field is sealed by stratigraphic facies changes to the West, and a lack of water influx coupled with the obvious

hydrocarbon saturations well below this level on E-logs suggest that the field is not in contact with any hydraulic pressure. Therefore, the OWC has been represented at a constant horizon of -1,000' from sea level datum.

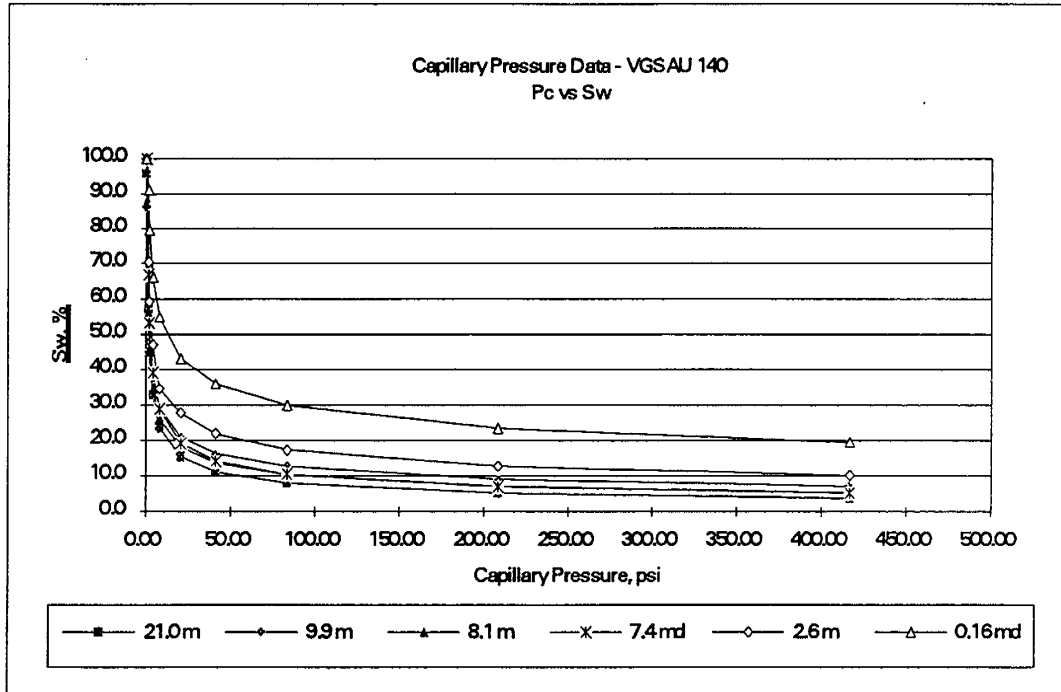


Figure 6: Capillary pressure related to water saturations, S_w . VGSAU Well No. 140.

Capillary pressure data is available for VGSAU Wells 140 and 157. VGSAU Well No. 140 had the only core centrifuge derived capillary data (air-water) available. Mercury injection derived capillary pressure data from VGSAU No. 157 was found to be of questionable value for these calculations. The mercury capillary pressure data was inconsistent from sample-to-sample. Capillary pressure data from VGSAU Well No. 140 is plotted in Figure 6. The laboratory data was then related to the height above zero capillary pressure (the OWC) by the following formula,

$$P_c = (\rho_o - \rho_w)h/144$$

where,

P_c	=	Capillary pressure, psia
ρ_o	=	Oil density, lbs/ft ³
ρ_w	=	Water density, lbs/ft ³
h	=	Height above $P_c = 0$, ft

The data was converted to reservoir conditions by applying the following scaling factor:

$$f = (\sigma \cos \theta)_{\text{air-water}} / (\sigma \cos \theta)_{\text{oil-water}}$$

where, f = Scaling factor, dimensionless
 σ = Interfacial tension between respective fluids, dynes/cm
 θ = Contact angle between respective fluids, degrees

[The products of the interfacial tension and cosine of the contact angle for the laboratory fluids (air-water) and the reservoir fluids (oil-water) were taken from Core Laboratory's Fundamentals of Core Analysis¹⁸, as 72 and 26, respectively. The resulting scaling factor is 2.77]

This capillary pressure data was used to determine the S_{wi} profile of the reservoir calculated at the geometric mean permeability. The geometric mean permeability of the VGSAU Well No. 140 core was found to be 2.7 md, which compared favorably with the geometric mean average for the entire Vacuum Core Database. The average S_{wi} determined by this approach was then estimated at 19.5 % for the main pay zone. The capillary pressure approach is considered to be within the limits of accuracy and is historically supported by log derived values of 20.0 % as the average S_{wi} within the pay.

The capillary pressure data was then reduced to a Leverett "J" Function, $J(S_w)$ with the following formula:

$$J(S_w) = h(\rho_o - \rho_w)(k/\phi)^5 / 144(\sigma \cos \theta)_{\text{oil-water}}$$

where, $J(S_w)$ = Leverett "J" Function, dimensionless
 ρ_o = Oil density, lbs/ft³
 ρ_w = Water density, lbs/ft³
h = Height above $P_c = 0$, ft
 σ = Interfacial tension between respective fluids, dynes/cm
 θ = Contact angle between respective fluids, degrees
k = Permeability, md
 ϕ = Porosity, decimal

The capillary pressure derived $J(S_w)$ data points for VGSAU Well No. 140 are shown in Fig. 7 along with the data points derived from the well's logging suite. For the wireline derived data, the porosity value was taken from wireline measurements, normalized to core porosity. The permeability was determined by neural network relationships derived from core porosity and core permeabilities discussed in detail elsewhere within this same report. A curve was fit to match this data, and is also provided in the same exhibit.

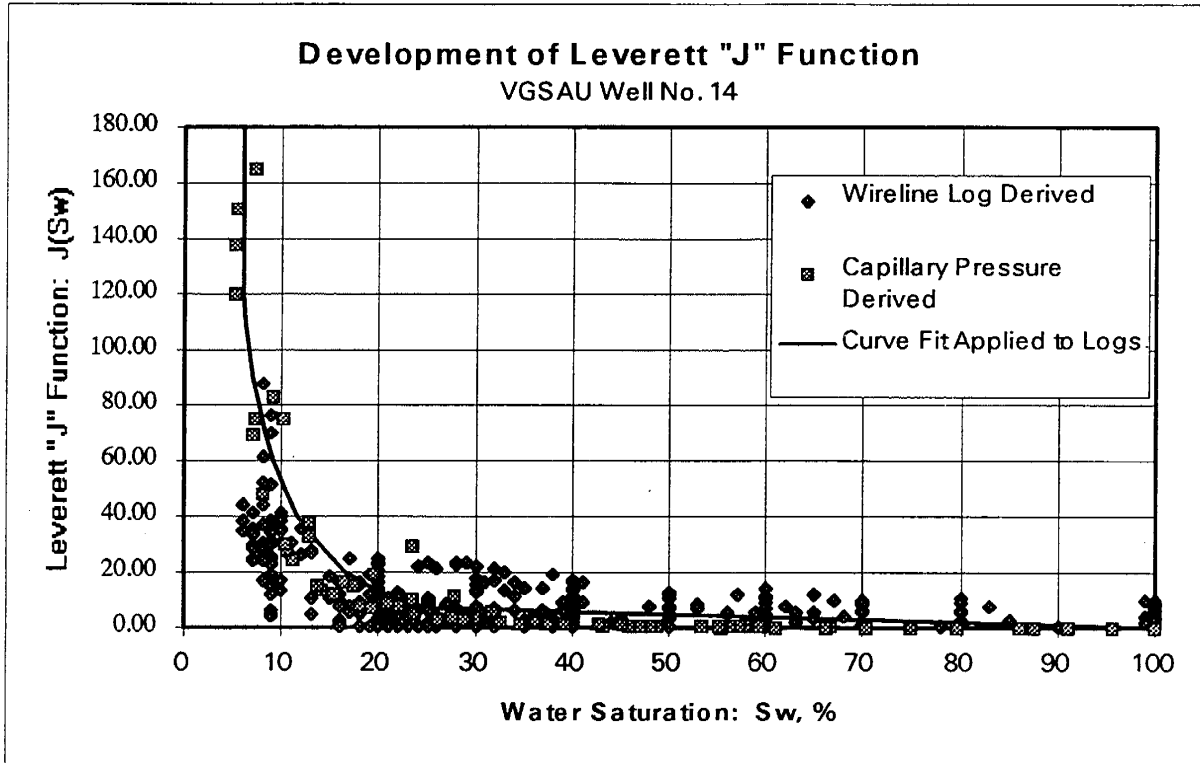


Figure 7: Comparison of wireline derived saturations and capillary pressure derived $J(S_w)$ data. VGSAU Well No. 140.

This curve-fit relationship is then applied to all wells within the study area to define the S_{wi} profile for the reservoir. The average water saturation, S_{wi} , for the pay zone in this same well using $J(S_w)$ results in a value of 20.9 %, further supporting previous findings. The $J(S_w)$ derived calculation is compared to the E-log values in Figure 8 for VGSAU No. 140.

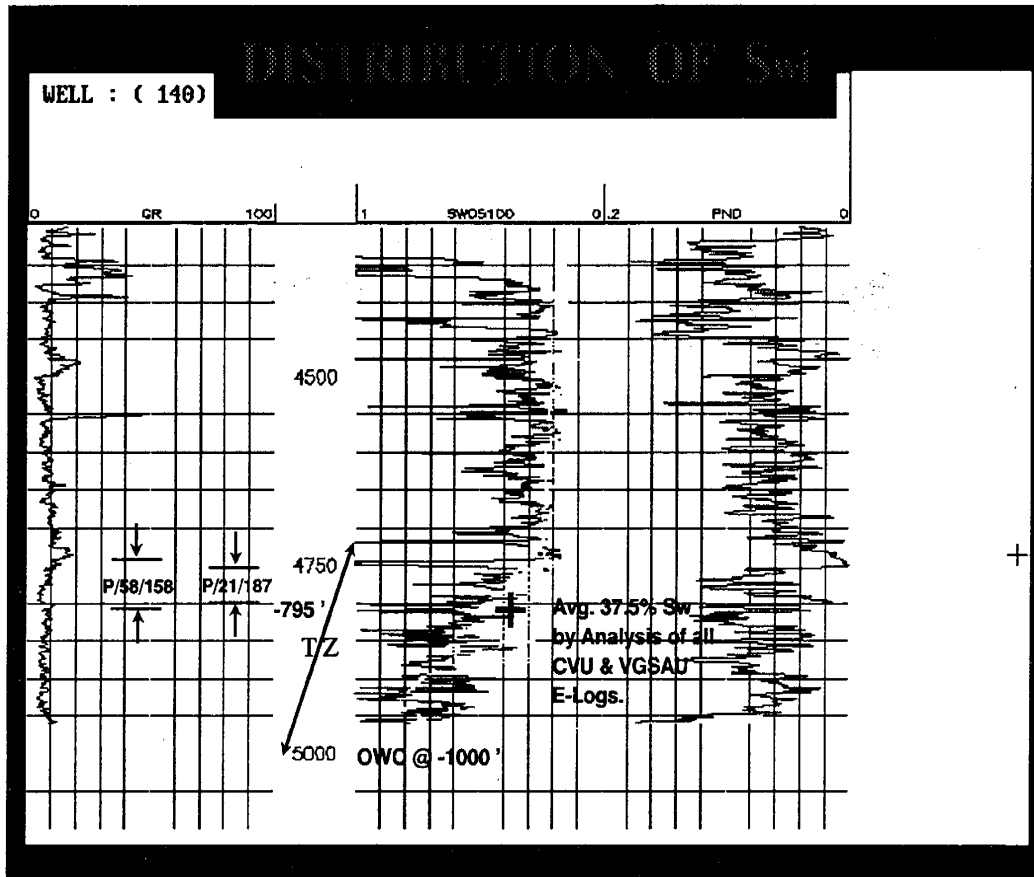


Figure 8: Leverett "J" Function developed S_{wi} profile compared to wireline data. VGSAU Well No. 140. Production tests tend to support definition of transition zone (however waterflooding has been active for 12 years). Evaluation of all electric logs available suggests that the Avg. 37.5% S_{wi} (50% water per fractional flow curve) is at -795' from sea level.

Application of this $J(S_w)$ also honors the fractional flow curve. Field production tests prior to waterflooding suggested that appreciable water production would not occur above -700' from sea level. Recent testing of individual deeper zones further suggests that 100.0 % water production should be expected below -800' from sea level. The fractional flow curve suggests 100.0 % oil flow below approximately 25.0 % S_w and 100.0 % water flow above approximately 60.0 % S_w . These two end points on the fractional flow curve are honored by application of the $J(S_w)$ derived above to log data.

A review of resistivity logs run before the introduction of foreign fluids to the reservoir suggests an S_{wi} as low as 15.0 % in some of the shallower, higher quality pay zones. This range is supported by the capillary pressure study. More recent resistivity measurements indicate S_{wi} as low as 6.0-10.0 % in some of these same correlative zones. This is likely a resultant of the introduction of fresh water to the system in the early years of waterflooding, along with continued fresh water make-up volumes added to the produced water prior to reinjection. In addition, a polymer augmented waterflood performed in the mid 1980's could have also adsorbed onto the matrix rock adding to the complexity of modern resistivity log interpretation.

The culmination of this exercise was the selection of a “pseudo-OWC” surface, or an “economically attractive OWC” within the TZ which would be used in the calculation of OOIP. However, with much consideration and review of data, it was felt that it was more important for this project that the OOIP be calculated to represent the hydrocarbon section available for application of the proposed technology. Therefore a detailed study of past and current completions identified a fairly constant surface at -700’ subsea to be the average bottom of the producing horizon. This artificial horizon will be used in subsequent evaluations of OOIP. The $J(S_w)$ relationship will be applied to the massive database described in the geostatistics section of this report for initial simulation model conditions. Material balance will allow estimation of current average saturations by injection pattern for waterflood efficiency review.

NET PAY DETERMINATION

It might have hydrocarbon saturation, but can it be produced? Not all reservoir rock is economically productive. It is important to know what reservoir pay is contributing to the production stream. Disregarding sweep efficiency, a 98.0% water-cut is reached just before 98% of the reservoir flow capacity is depleted. Therefore, as a rule-of-thumb, the 98.0% flow-capacity has been used in considering the permeability cutoff. By sorting the database on permeability, the permeability necessary to provide 98.0% flow capacity (k^*h) can be determined. Noting the corresponding storage capacity (Φ^*h), the database is resorted on porosity, Φ . The porosity cutoff corresponds to the same value of storage capacity found in the previous sorting. Use of either the porosity or permeability cutoff should yield approximately the same value for net pay.

A total of 18 whole-core analyses (10 CVU & 8 VGSAU) provided 4,312 porosity and permeability samples, representing 4,979’ of reservoir material for study. The data was digitized for database manipulation. Fracture dominated footage was culled, along with any “plug” analyses. Evaluation of the database finds on average a 1.7 md permeability cutoff within the oil column to be equivalent to the 98.0% flow capacity, which corresponds to approximately a 7.0% porosity cutoff. Each of the zones identified within the reservoir was evaluated independently. The findings are included in Table 1.

Table 1: RESULTS OF POROSITY & PERMEABILITY CUTOFF STUDY

ZONE	FOOTAGE AVAILABLE, ft	PERMEABILITY CUTOFF, md	POROSITY CUTOFF, %	Avg. POROSITY Above CUTOFF, %
Grayburg Dolomite	320	0.8	7.3	10.2
Grayburg Sandstone	256	0.4	7.3	11.4
Upper San Andres	1,823	2.7	7.9	12.0
Lovington Sandstone	211	0.1	5.0	7.1
Lower San Andres	2,368	1.5	7.3	11.3
TOTAL	4,979	1.7	7.7	11.6

The sandstone intervals are considered to be non-pay. Where sandstone porosity is developed, the permeability is inferior to the carbonates of the Grayburg and San Andres dolomite. The

Grayburg Sandstone is believed to contain a considerable amount of samples interbedded with carbonate material which inflates the findings. The Grayburg Sandstone is similar to the Lovington Sandstone. The overall flow capacity of the producing horizon is not likely effected by the sandstones. However, no capillary pressure data has been gathered to confirm this assumption. No known production tests of the sandstone interval have been found.

A cutoff value for porosity in the 7.0% range seemed high. As a confidence check, an entire set of East - West row injection well profiles within the study area was reviewed. No single zone below 7.0% porosity was accepting water based on the velocity and tracer surveys available. One of the injection wells also had a production profile log dated prior to its conversion. It did not indicate any production from zones below 7.0% porosity (but we should keep in mind that production profiles are typically run because production anomalies exist).

A study of vertical permeability was conducted. Only two wells included any measurements of vertical permeabilities. The ratio of vertical-to-horizontal permeability was found to be 0.30:1.00 and 0.27:1.00 for the VGSAU Well No. 140 & 157, respectively. The sandstone intervals were excluded from the analysis. Although these ratios seem fairly conductive, it is suspected that the effective vertical transmissibility between facies in a heterogeneous carbonate reservoir is negligible.

PERMEABILITY RELATIONSHIPS

A more descriptive characterization of a reservoir would include a variance in permeability rather than the application of an average value. Permeability relationships provide a method of distributing saturations and evaluating flow capacity; an integral need for reservoir simulation. Past work has involved the use of linear regressions to represent a scattering of core measured porosity vs. permeability data.

This portion of the reservoir characterization applies artificial intelligence to determine porosity/permeability relationships and then derive values of permeability for all well traces in the study. The use of a neural network to derive permeability from wellbore measurements is a patented Texaco process (Patent number 5,251,286, October 5, 1993, "Method for Estimating Formation Permeability from Wireline Logs using Neural Networks"). Further information concerning the patent can be obtained from Jack Wiener c/o Texaco E & P Inc., P. O. Box 2100, Denver, CO 80201-2100 (DD: 303-793-4079).

Artificial intelligence is a name applied to several types of computer programs which attempt to simulate the decision making processes of a human. The particular type of artificial intelligence applied to develop the porosity/permeability relationship for this project is called a neural network. A neural network is made up of number highly interconnected individual processing units much like a mamalian brain is made up of a very large number of highly interconnected neurons. Neural networks consist of input nodes, where data is supplied to the network, and output nodes where resulting values are generated. Between these two sets of nodes are one or more "hidden" layers of nodes. Every input node is connected to every hidden node. Every hidden node is connected to every output node. Every one of these connections has an

independently associated weight factor. The artificial intelligence of neural network is a found in two places. The first is the knowledge of the relationship between inputs and outputs is represented by the values taken on by the weight factors. It is these values and how they are interconnected that shows why this branch of artificial intelligence is called neural networks. The second is how the neural network acquires its knowledge of the relationship between inputs and outputs. With typical computer programming the relationship is coded directly into the computer program by a human. With a neural network there is no *a priori* knowledge of this relationship. The neural network must create its own coded program which captures the relationship between inputs and outputs. This is done by having the neural network learn the relationship by repeatedly comparing examples of inputs with their associated outputs and self-adjusting the connection weights until it has developed a relationship that works. After the neural network has learned the relationship between inputs and outputs it is ready for use. This phase of the operation is to present the input nodes with data in which the values of the outputs are unknown, and let the network solve/generate, based on the results of the learning phase, for the unknown values. Commercial software is available for designing and applying neural networks. For this study, NeuroShell, a product of Ward Systems Group, Inc., and NeuralWorks, a product of NeuralWare, Inc. were used.

The data set supplied to the network during the learning phase included porosity and permeability values derived from core measurements obtained from eighteen wells (aerial distribution) within the project area. This core data were reviewed for evidence of fracturing, and suspect data were culled from the data set. This left slightly over 4,000 data points to be used in training the network. Additional data from the core included its physical location, latitude and longitude, and macro-zone identification.

The general methodology used for this study consists of four steps;

1. Decide what data to use to train the network and assemble it in the proper format.
2. Present the data to the network and allow "learning" to occur.
3. Apply the network to a test data set held in reserve for this purpose.
4. Evaluate the effectiveness of the network.

After the above steps are complete, a decision is made as to what changes to the network architecture or the training data set would most likely improve the performance of the network, and the methodology is repeated until the resultant network gives satisfactory performance. More than fifty repetitions of the above process were completed before a network was finalized to apply to the wellbore data. Several findings are of note in the case of this study:

1. Any input data used to train the network, must also be available for all data points to be analyzed (for instance, if sonic travel time is used to train the network, then sonic data will be required to apply the network).

2. A major hurdle to the application of neural networks in mature fields such as Vacuum is the lack of consistent usable data from well-to-well. The "lowest common denominator" of data for this project was normalized wireline porosity, location of the well in latitude and longitude, and macro-zonation of the reservoir. Better results could certainly have been achieved if, for example, sonic logs and resistivity logs had been available for all wells, or pore-type descriptions.

3. In spite of the limitations in data cited above, the final neural network achieved a mean absolute deviation (error) of 7.28 millidarcies vs. 10.96 millidarcies for the standard linear regression analyses. In this case, the application of standard linear regression analysis would have resulted in data 50% less accurate than that obtained from the neural network.

Figure 9 is a scatter-plot of porosity vs. permeability on a semi-log plot for a representative test set of the core data and the neural network solution. Although not perfect, it exceeds the historical option of linear regression considerably. Permeability not only varies with porosity, it also varies spacially over the study area within given zones due to the nature of the geology of the area as represented in the training set.

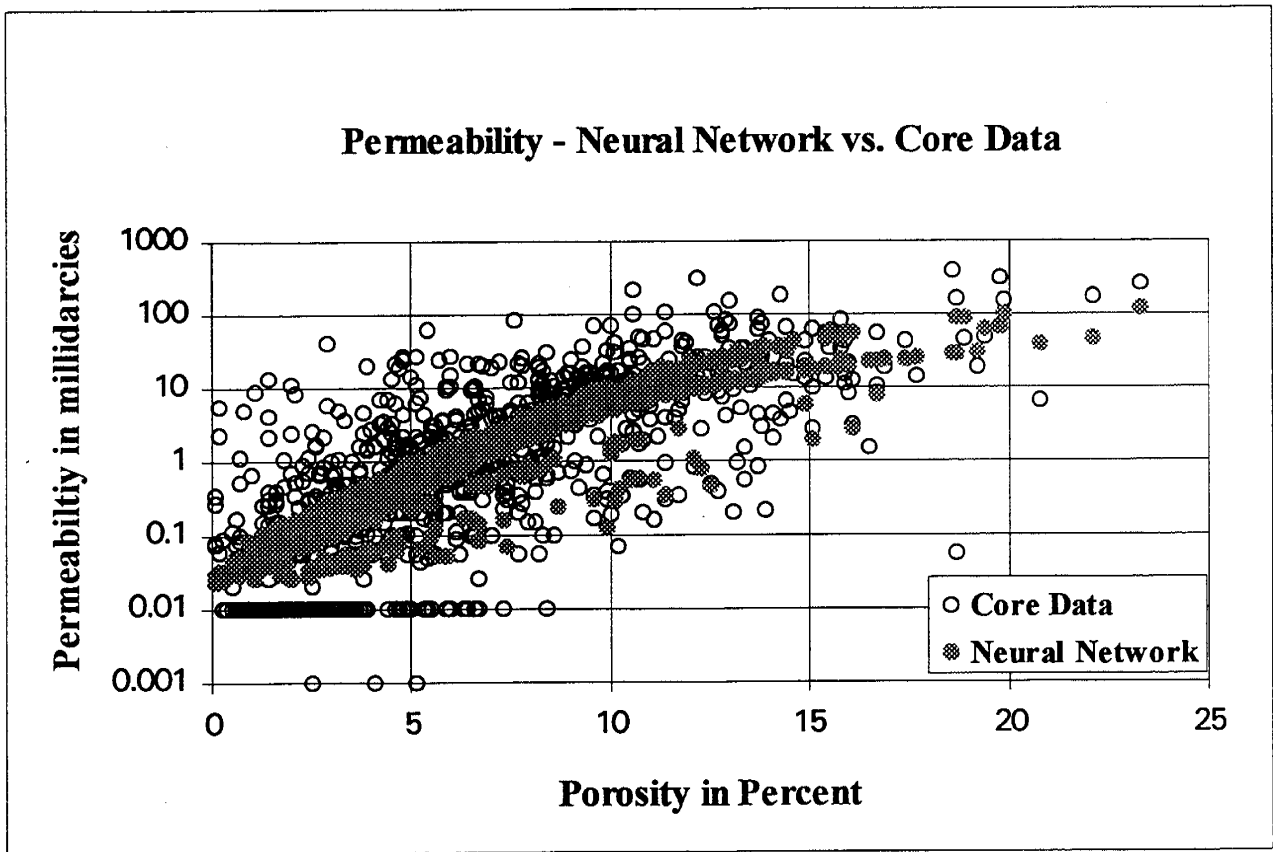


Figure 9: Neural Network Solution of permeability relationship to porosity. Example for well (test set) VGSAU No. 140.

GEOSTATISTICAL REALIZATIONS

Once a permeability relationship is obtained through the use of neural networks, another problem is interpolating the data between well locations. Core data shows that porosity and permeability can vary by orders of magnitude over a small interval. If this is any indication of the variability or heterogeneity that exists between wells, then methods are needed to incorporate this in reservoir models. Geostatistics has been used in this study to distribute wellbore data to interwell locations (cells). This exercise is believed to have provided a more realistic spacial distribution of the data than the typical algorithm used in mapping software. Normalized porosity and neural network derived permeability data from 455 wells in the project area were available for use. Markers within the pay were taken from the project database.

The first step involved screening data. All sonic logs were removed from the population. It was felt that the sonic logs were introducing statistical variation. This effect was the result of differences in the ability to recognize secondary porosity. The neutron derived logs would see the secondary porosity. The normalization techniques used on these different logging suites resulted in a poor sonic-core porosity relationship, which will be addressed at a later time. The reduced well count used for the variograms and gridding was 322.

Initial porosity variograms appear reasonable. The Grayburg Dolomite has its greatest correlation trend in a north-northeast to south-southwest direction. The Grayburg Sandstone and the San Andres have their greatest correlation trend in an East to West direction. Not surprisingly, this trend follows the strike of the basin margin.

At 752,400 cells, the geostatistical exercises are handling a rather large volume of data for the study. The 3-D gridding consists of 150 layers within the San Andres formation, with an aerial distribution of 76 rows, by 66 columns. The layers are 4.00 ft thick. Each cell is 250 ft X 250 ft on a side. This work is being performed on a personal computer with a geostatistical software package developed by Texaco, called GRIDSTAT. Preliminary 3-D porosity grids have been created using a kriging gridding algorithm. In the case of this project, the model area had to be broken into sections due to its size. After working with several grid generations, it became obvious that the software was not properly using the data from wells in adjacent sections--resulting in "banding." The software coding was subsequently refined and the banding problems eliminated. An acceptable porosity grid for the project area has now been defined for the San Andres formation. Final tasks will involve the generation of improved geostatistical grids within the overlying producing horizons of the Grayburg formation.

Originally, it was anticipated that the variograms developed from the porosity data would be used in construction of the permeability grids. This approach has been abandoned in favor of directly applying the neural network permeability relationships corresponding to the geostatistically distributed porosity. The original approach left concern regarding the redistribution of permeability data which was partially defined based on its 3-D spacial distribution in the reservoir. Therefore, efforts are underway to apply the neural network to this massive porosity grid. Figure 10 visually depicts the process of dealing with this large mass of data. The porosity values are

first downloaded from Stratamodel or GRIDSTAT, to an ASCII file format, and imported into an Access database. Cell location (latitude & longitude) not available in the original databases, are added to the Access database. The previously trained Neural Network is then applied to calculate “virtual” permeabilities for each of the cells. The data can then be uploaded to Stratamodel for visual inspection.

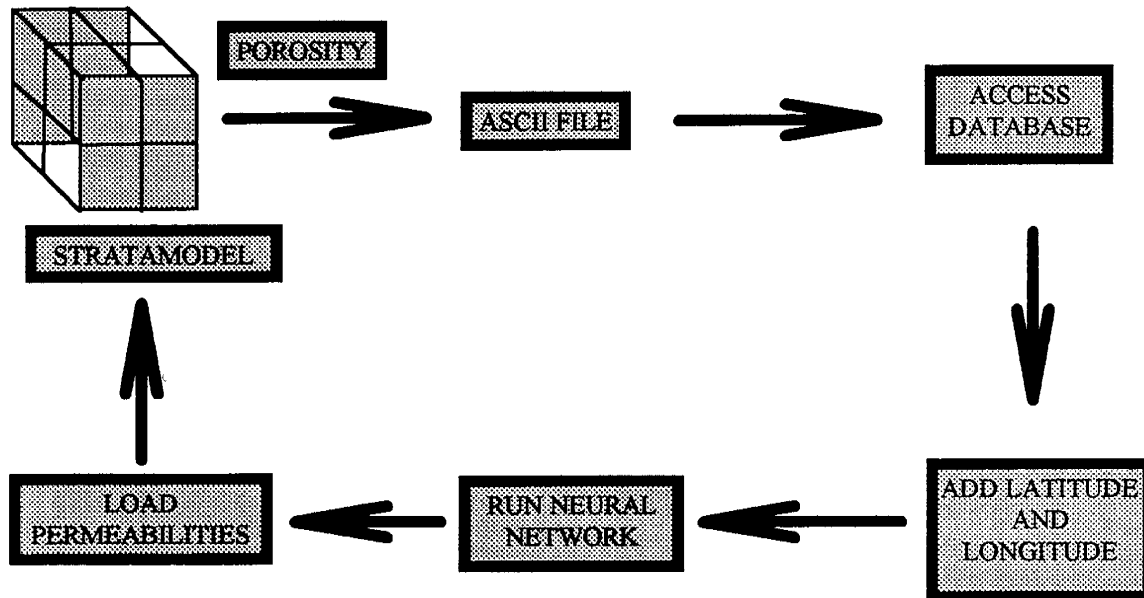


Figure 10: Visual depiction of data management associated with assignment of permeability to porosity grid cells.

The 250' X 250' aerial grids are being used to determine saturations throughout the entire field study area. Work is underway to define the grid requirements for the smaller site specific simulation model. The coarser grid of the field will not allow the detail needed for the compositional simulation model. Further, the detailed grid would be prohibitively large for the field review requirements. The intent is to avoid any averaging of kriged data within the simulation model. Grid size optimization is proceeding while considering limits imposed by the compositional simulation. The end product must support the simulation process.

Conditional geostatistical simulations will be performed on the site specific model area in conjunction with the parametric simulation tasks. An evaluation will be made to determine if the porosity variograms constructed from the field wide data are applicable to the site specific model area prior to kriging and conditional simulations.

WATERFLOOD REVIEW

A review of waterflood efficiencies has been initiated. It is anticipated that this detailed review will allow proper selection of the eight sites for the field demonstration of the proposed technology. The results of the parametric simulation studies will be coupled with the waterflood review information. The intent is to be able to select a sufficient variation in reservoir

conditions/character to support the parametric studies findings. Guidelines will ultimately be developed to assist operators in selecting candidate sites based on this information and actual field trials.

The study is currently limited to evaluation of effects not related to OOIP since the final figures will not be available until completion of the geostatistical exercises mentioned previously. However, review of various relationships are progressing. No abnormalities in these initial studies are suggested.

Based on the cursory review of currently available data, a site specific model area has been selected. It is located in the northern area of Section 6, T18S - R35E, Lea County, New Mexico. This model area represents average reservoir conditions known to exist within the study area. It includes four (4) existing 40-acre 5-spot injection patterns. The size of the model will allow for the potential to analyze results from more than one field demonstration. This configuration was selected as a safety precaution, should the initial site fail mechanically. This model area is currently being drilled on a higher density well spacing -- providing modern logging suites. This data will help refine the model and provide a measure to the geostatistical efforts. The drilling is not part of the cost-share DOE project.

DEVELOPMENT OF AN EQUATION-of-STATE

Western Atlas' DESKTOP-PVT program has been used to develop an Equation-of-State (EOS) which will be incorporated in the compositional simulations for the CVU H-n-P process.

Constant composition expansion experiments had previously been run in 1989 on samples of CVU crude oil (CVU Well No. 162) with increasing concentrations of CO₂¹⁹. Concentrations of 0, 20, 41, and 55 mole-% CO₂ resulted in bubble point fluids. Liquid phase viscosities were determined for the 0, 41, and 55 mole-% CO₂ samples. Concentrations of 70, 75, and 85 mole-% CO₂ did not result in dew point fluids. No single phase was formed below 6,000 psia (equipment limitation) for any of these last three mixtures. Phases included a CO₂ rich vapor (V), a hydrocarbon rich dark liquid (L1), and a CO₂ rich clear liquid (L2). Below 1,158 psia, V and L1 are present and above 1,316 psia, L1 and L2 are observed. Between these two pressures all three phases are present. Since compositional simulators are limited to two-phase equations of state, approximations were required to deal with the three-phase behavior observed in the laboratory experimentation.

The CO₂ rich liquid phase, L2, present above 55 mole-% CO₂ and 1,158 psia was treated as part of the vapor phase. Above 55 mole-% CO₂, saturation pressures could not be determined and were estimated. Given the error inherent in these estimates, the relative volume (sample volume at given pressure divided by volume at saturation pressure) was not used as data to be matched. The heavy liquid phase (L1) fraction was the only data matched above 55 mole-% CO₂.

Prior to matching the experimental data, the C₇₊ fraction of the crude analysis (molecular weight of 202) was split into three pseudocomponents. In order to reduce the number of components and thus the run-time of the compositional simulation, the small amount of nitrogen was combined

with the methane, C₁, and the C₅ and C₆ components were combined. The system, shown in Table 2 was thus represented with nine pseudocomponents including CO₂.

Table 2: PSEUDOCOMPONENT SYSTEM

Original Components	Pseudocomponent	Mole-%
CO ₂	CO ₂	2.03
CH ₄ , N ₂	C1N2	14.19
C ₂ H ₆	C2	9.83
C ₃ H ₈	C3	9.80
nC ₄ H ₁₀ , iC ₄ H ₁₀	C4	8.38
nC ₅ H ₁₂ , iC ₅ H ₁₂ , C ₆ H ₁₄	C5C6	9.04
C ₇ +	HVY1 (MW=133)	27.21
C ₇ +	HVY1 (MW=251)	15.29
C ₇ +	HVY1 (MW=467)	4.23

A three parameter Peng-Robinson EOS was initially used to match this data and to provide CO₂ - Oil phase behavior descriptions for use in the compositional simulation model. The Omega A and Omega B EOS parameters for the three heaviest pseudocomponents, and the binary interaction parameters between these pseudocomponents and CO₂ were adjusted to fit the experimental phase behavior data. To insure proper CO₂ densities over the range of pressures anticipated in the CVU project, the CO₂ volume shift parameter was adjusted. A completely satisfactory match of the liquid volume fraction at high mole-% CO₂ mixtures could not be found with the Peng-Robinson EOS. Matching efforts were then shifted to the Zudkevitch-Joffe-Redlich-Kwong (ZJRK) EOS. The same EOS parameters were adjusted. Much better matches of the liquid volume fraction at high mole-% CO₂ mixtures were found with the ZJRK equation than with the Peng-Robinson equation. Typically the most difficult type of data to match is the liquid volume fraction for the high mole-% CO₂ mixtures. Viscosities were matched by adjusting the critical z-factor of the three heavy components in the Lohrenz-Bray-Clark viscosity correlation.

Table 3: CO₂ - OIL MIXTURE SATURATION PRESSURES

Mole-% Added CO ₂	Experimental Saturation Pressure, psia	Calculated Saturation Pressure, psia
0	790 BP	810 BP
20	1,045 BP	1012 BP
41	1,273 BP	1,241 BP
55	1,378 BP	1,405 BP
70	>6,000	3,263
75	>6,000	4,559
85	>6,000	10,042

A reasonable match of the bubble points for the 0, 20, 41, and 55 mole-% CO₂ mixtures resulted, as shown in Table 3. An excellent match was obtained for the relative volume as a function of pressure, the easiest property to match. Very good matches of the liquid volume fraction at 55 mole-% and below CO₂ mixtures were found. Good matches were found for the volume fraction for the high mole-% CO₂ mixtures (i.e., 70, 80, and 85 mole-% CO₂ mixtures). Satisfactory matches were also found for the viscosities. In addition, a reasonable match of pure CO₂ densities over the range of pressures likely for the project was found.

The match of CO₂ density is not standard and required a special procedure. The special procedure involved simultaneously matching pure CO₂ densities along with the laboratory CO₂ - oil phase behavior data. This was done because it was found that an EOS does not typically predict pure CO₂ density sufficiently well when it is matched only to the laboratory CO₂ - oil phase behavior data. When pure CO₂ density was also included in the matching process, the prediction of pure CO₂ density was much improved without significantly degrading the liquid volume fraction matches. Proper matching of CO₂ density is important for determining the amount of CO₂ used in a process. The EOS matches to the laboratory data are presented in Figures 11 through 25.

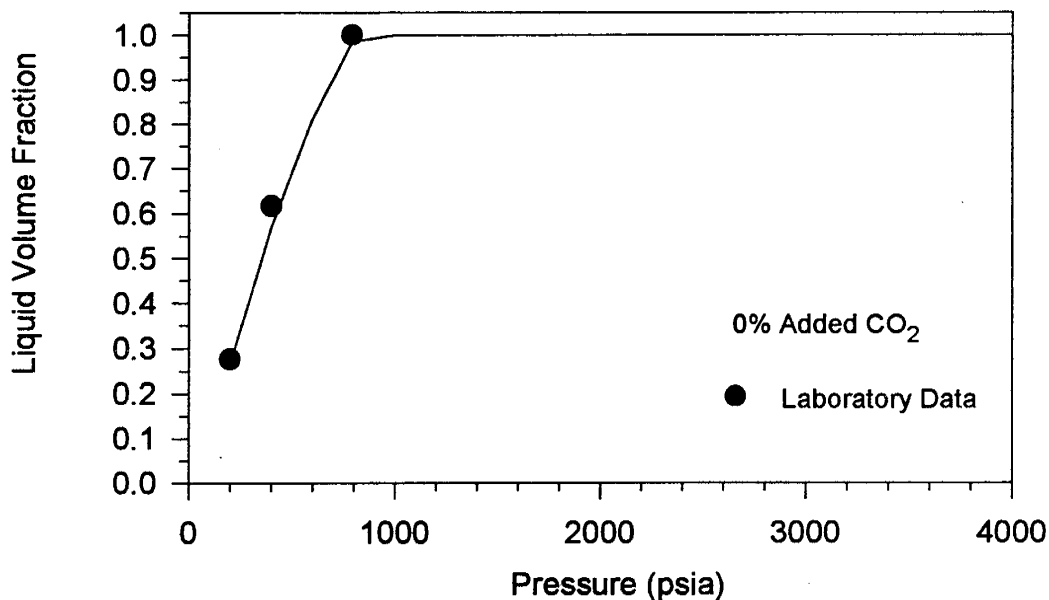


Figure 11: Comparison of laboratory data and EOS prediction of liquid volume fraction as a function of pressure for no added CO₂. (Solid line is EOS prediction)

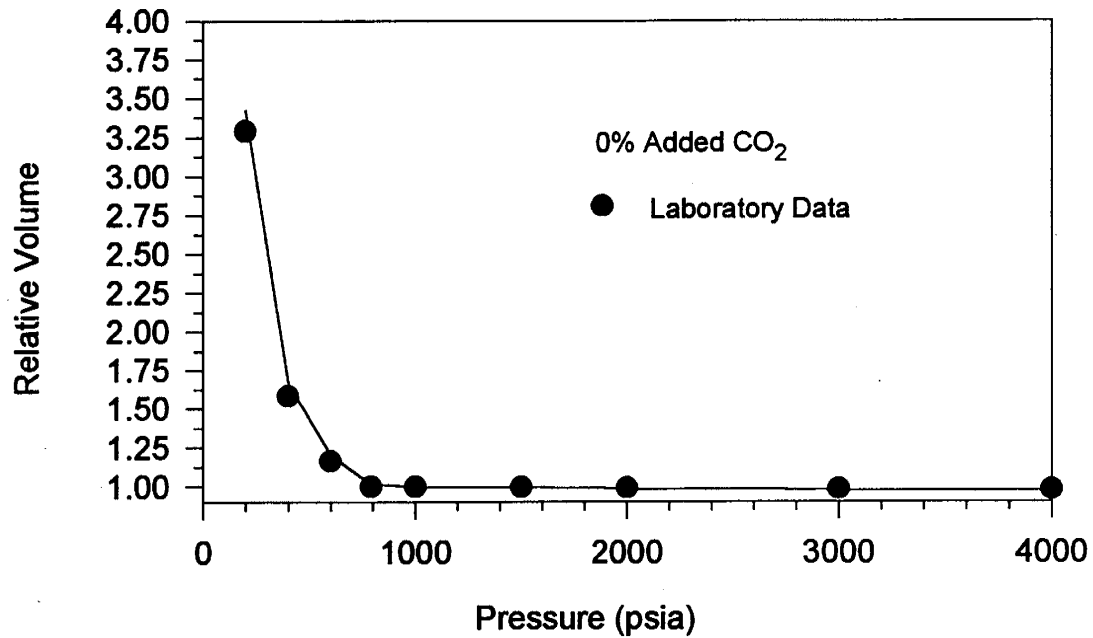


Figure 12: Comparison of laboratory data and EOS prediction of relative volume as a function of pressure for no added CO₂. (Solid line is EOS prediction)

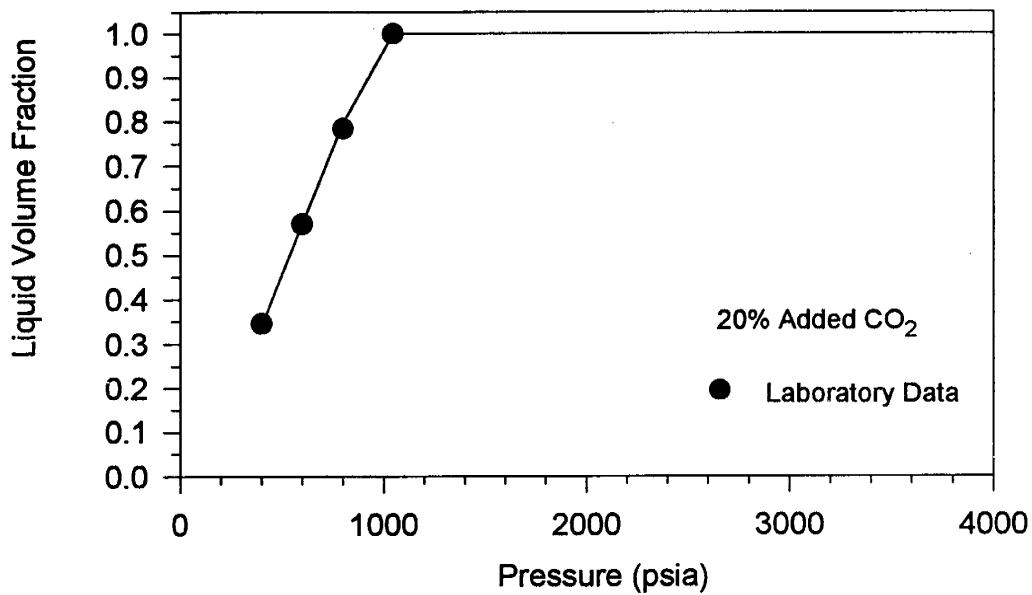


Figure 13: Comparison of laboratory data and EOS prediction of liquid volume fraction as a function of pressure for 20 mole-% added CO₂. (Solid line is EOS prediction)

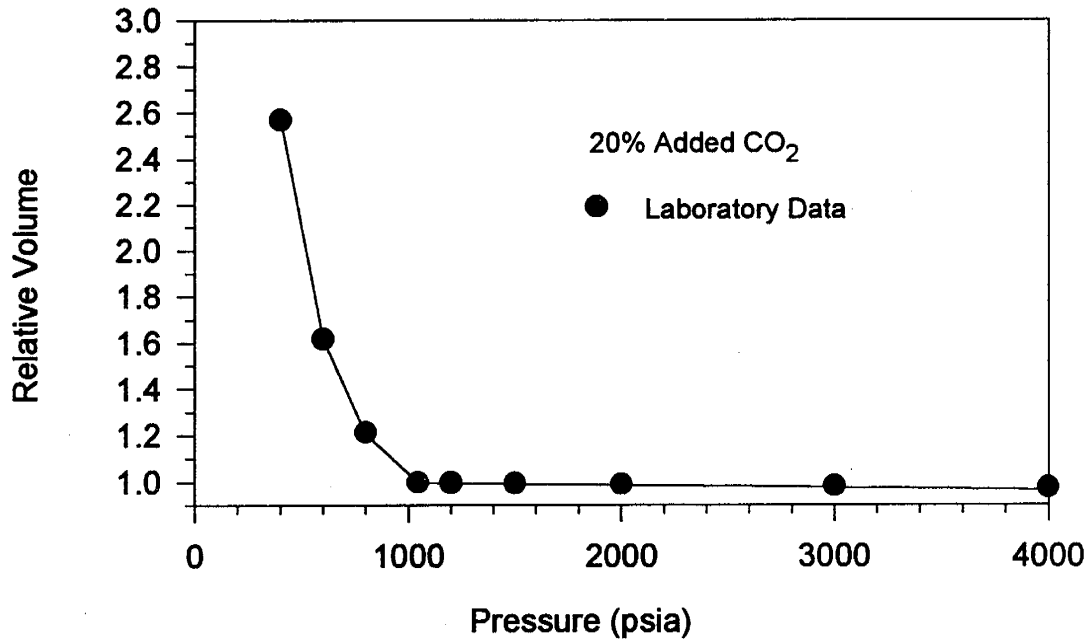


Figure 14: Comparison of laboratory data and EOS prediction of relative volume as a function of pressure for 20 mole-% added CO₂. (Solid line is EOS prediction)

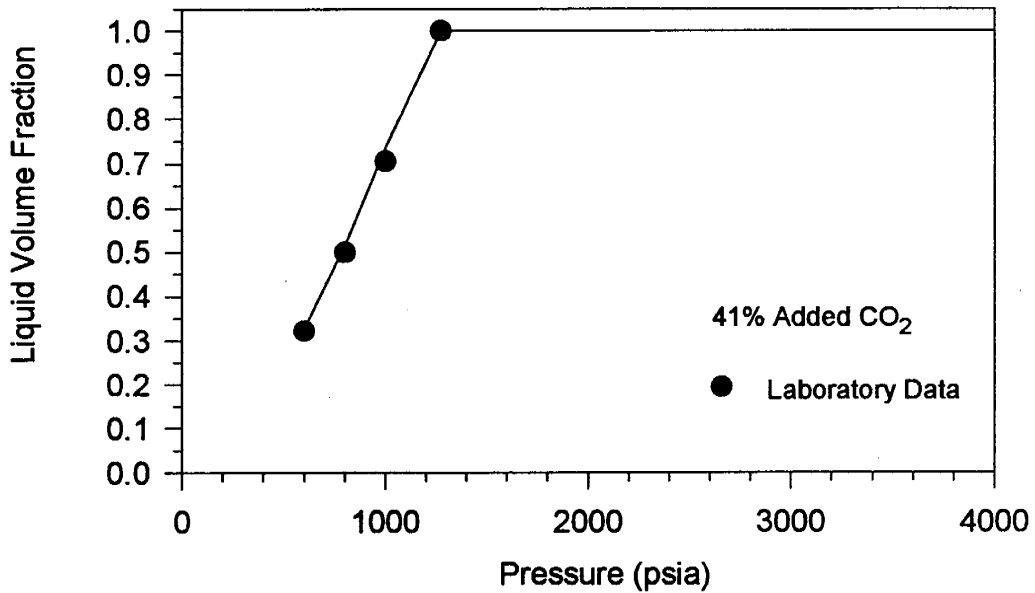


Figure 15: Comparison of laboratory data and EOS prediction of liquid volume fraction as a function of pressure for 41 mole-% added CO₂. (Solid line is EOS prediction)

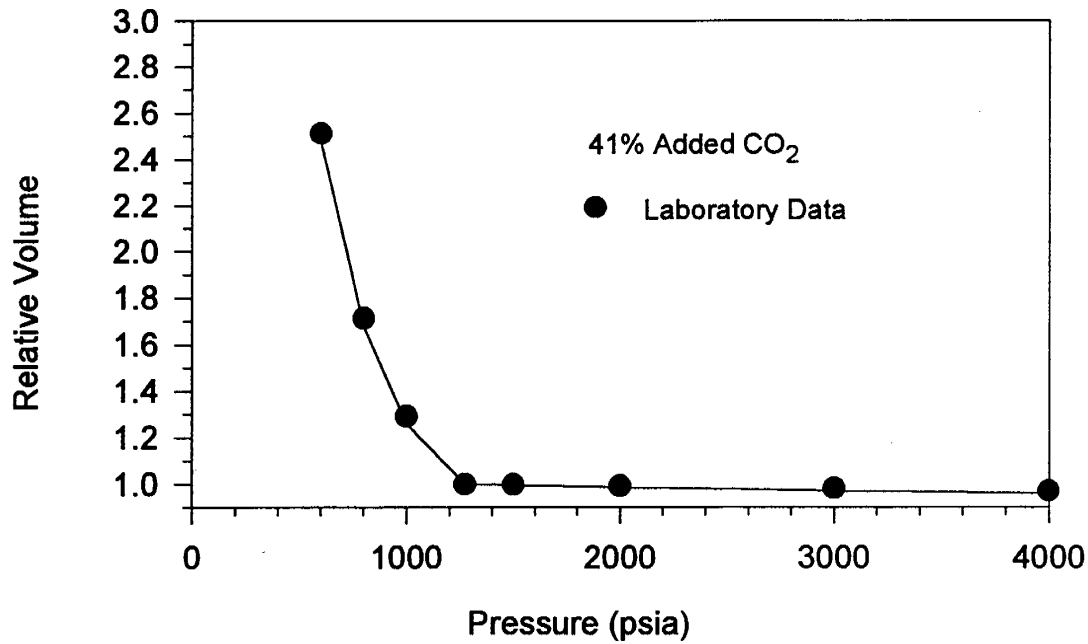


Figure 16: Comparison of laboratory data and EOS prediction of relative volume as a function of pressure for 41 mole-% added CO₂. (Solid line is EOS prediction)

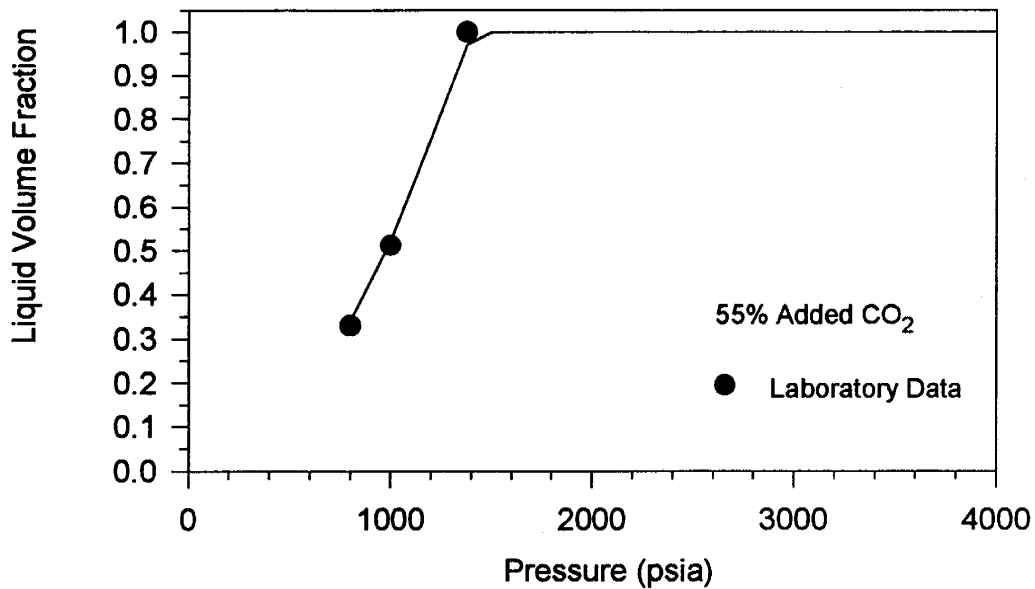


Figure 17: Comparison of laboratory data and EOS prediction of liquid volume fraction as a function of pressure for 55 mole-% added CO₂. (Solid line is EOS prediction)

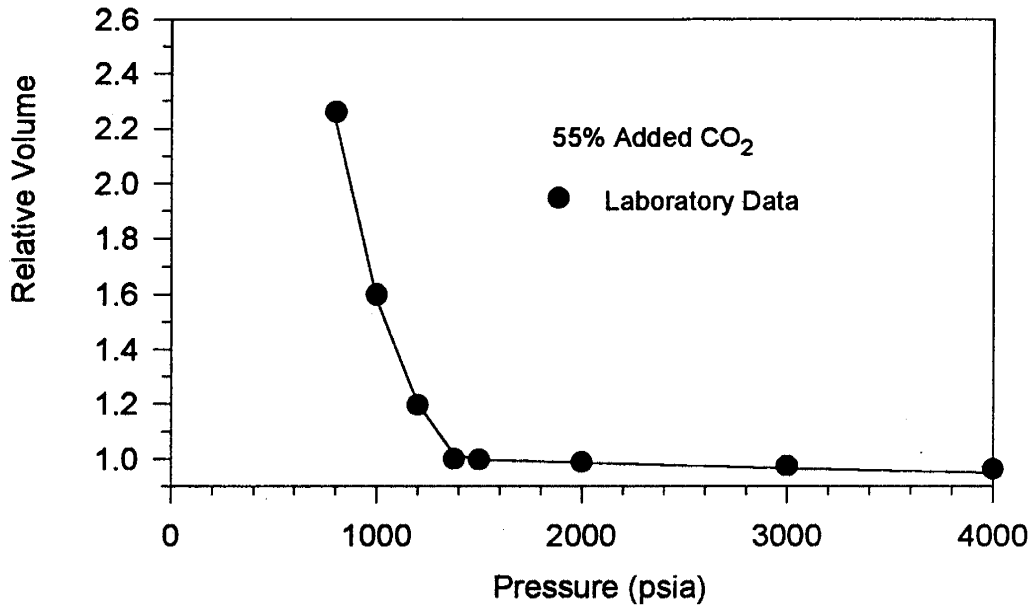


Figure 18: Comparison of laboratory data and EOS prediction of relative volume as a function of pressure for 55 mole-% added CO₂. (Solid line is EOS prediction)

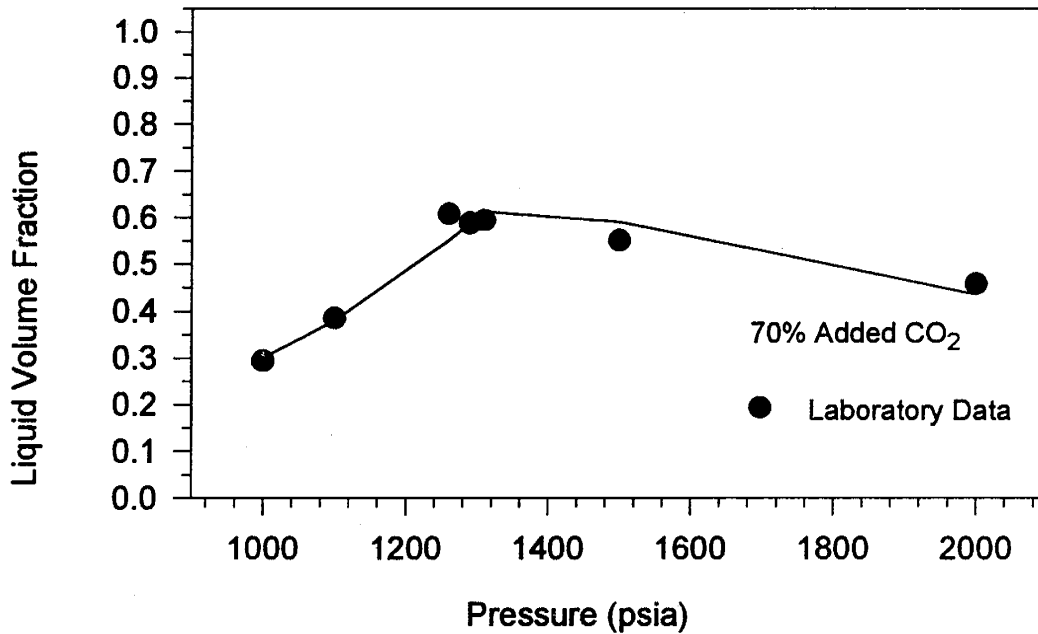


Figure 19: Comparison of laboratory data and EOS prediction of liquid volume fraction as a function of pressure for 70 mole-% added CO₂. (Solid line is EOS prediction)

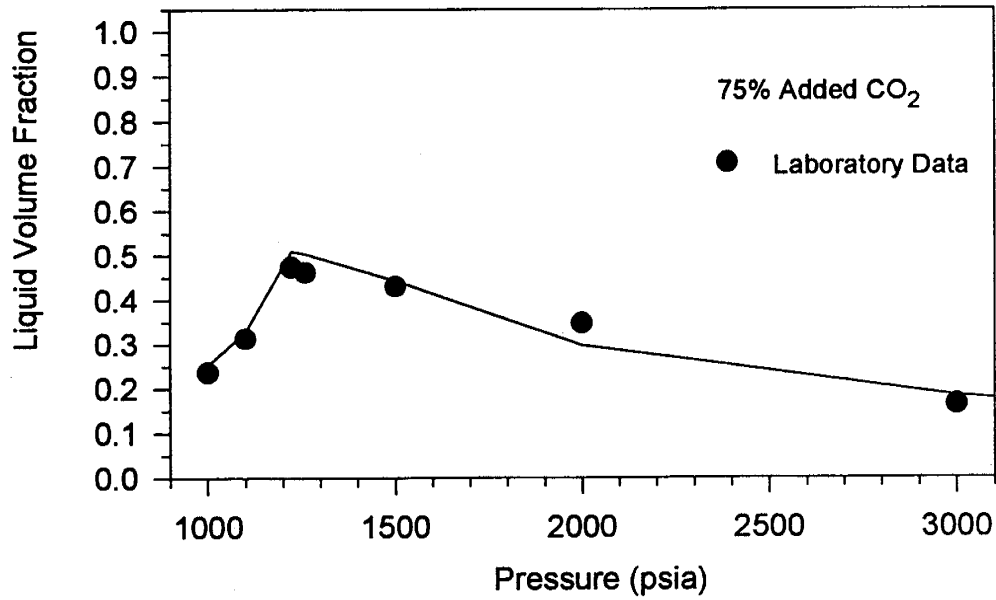


Figure 20: Comparison of laboratory data and EOS prediction of liquid volume fraction as a function of pressure for 75 mole-% added CO₂. (Solid line is EOS prediction)

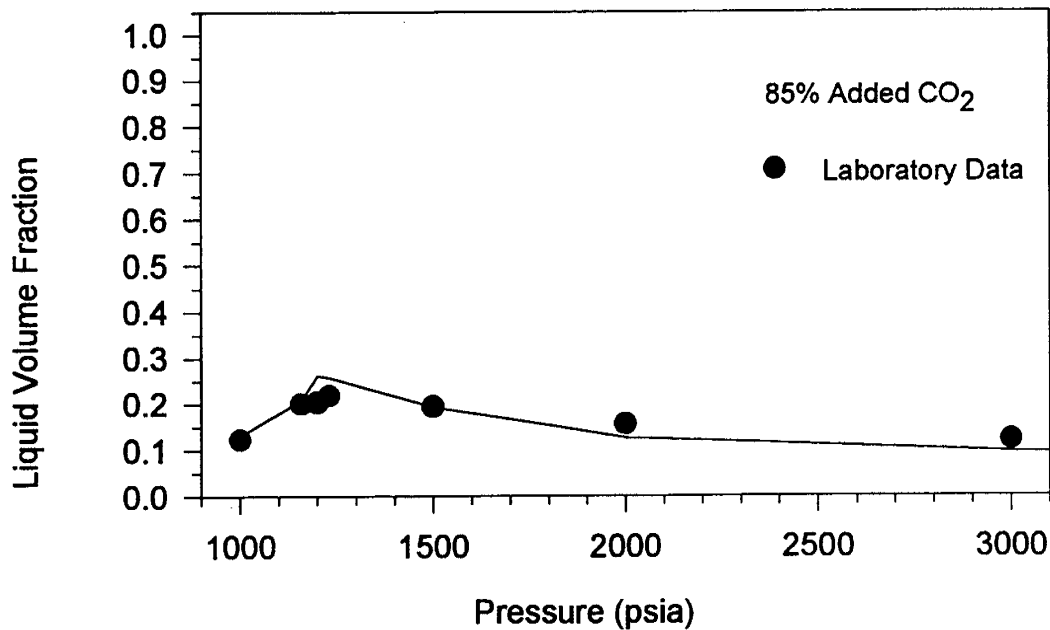


Figure 21: Comparison of laboratory data and EOS prediction of liquid volume fraction as a function of pressure for 85 mole-% added CO₂. (Solid line is EOS prediction)

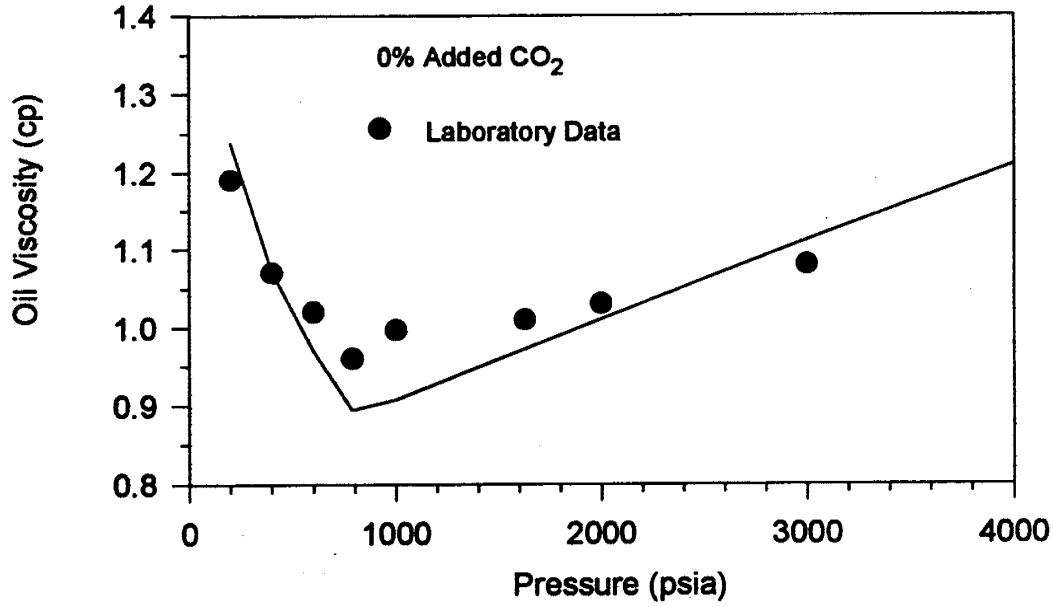


Figure 22: Comparison of laboratory data and EOS prediction of liquid viscosity as a function of pressure for no added CO₂. (Solid line is EOS prediction)

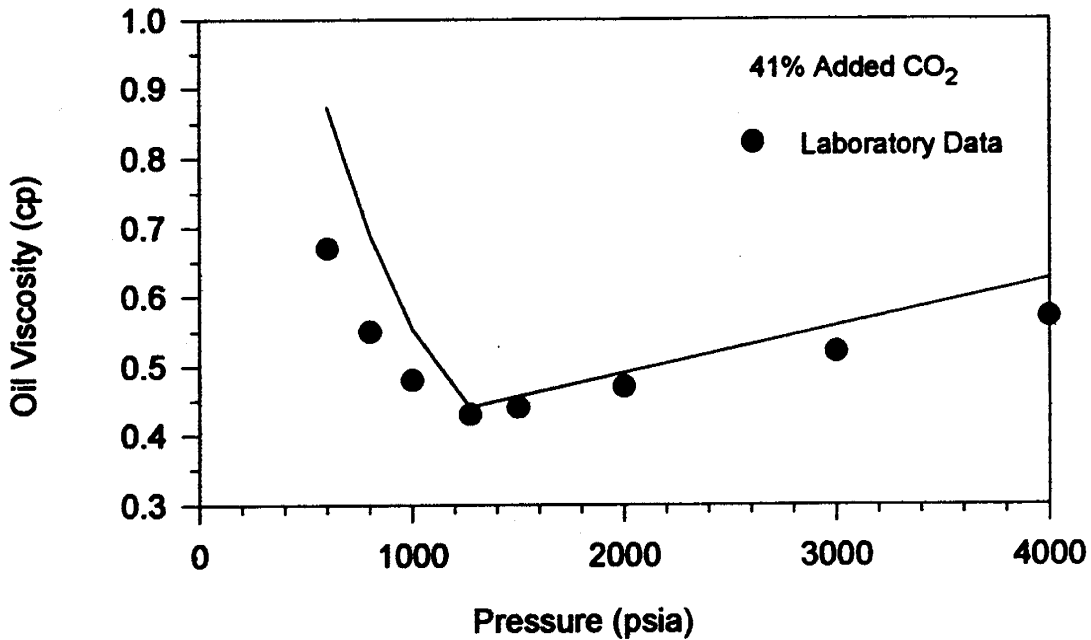


Figure 23: Comparison of laboratory data and EOS prediction of liquid viscosity as a function of pressure for 41 mole-% added CO₂. (Solid line is EOS prediction)

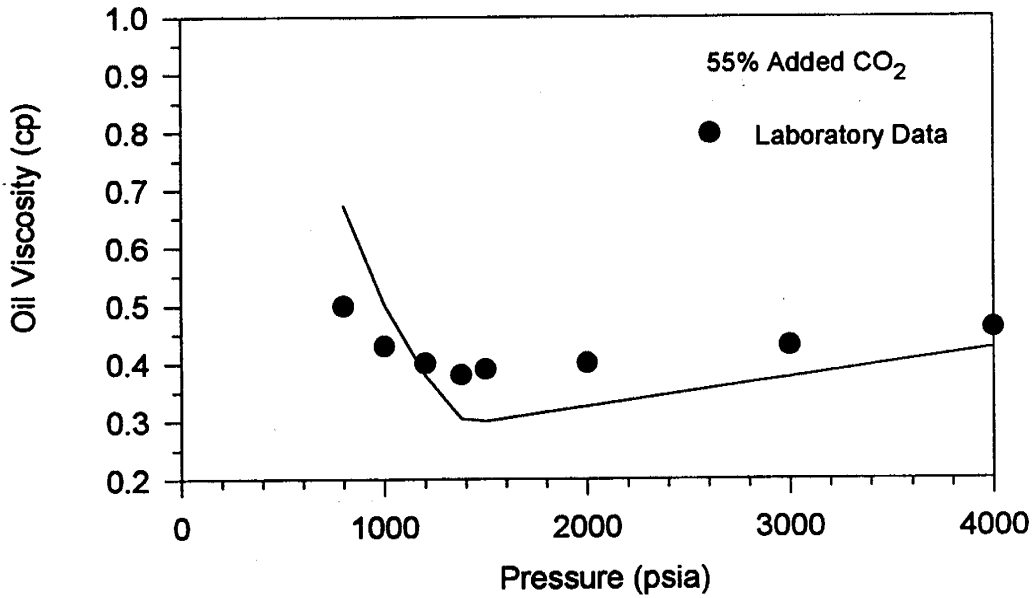


Figure 24: Comparison of laboratory data and EOS prediction of liquid viscosity as a function of pressure for 55 mole-% added CO₂. (Solid line is EOS prediction)

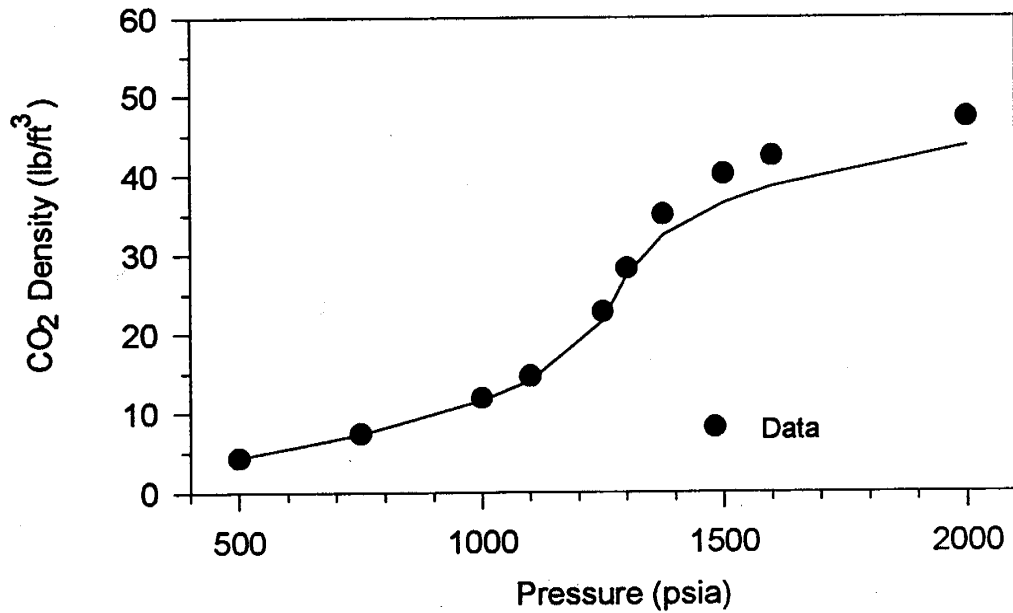


Figure 25: Comparison of established data and EOS prediction of pure CO₂ density as a function of pressure. (Solid line is EOS prediction)

Slimtube experiments were performed in 1989²⁰. The tests were conducted at a temperature of 105° F and from 1,100 through 3,000 psia to determine the CVU crude system's minimum

miscibility pressure (MMP). The MMP was found to be approximately 1,250 psia. Considering the complexity of dealing with the three phase system, simulations of these laboratory experiments were necessary for the development of a realistic fit of the live oil - CO₂ phase behavior data. The slimtube experiments were successfully simulated with the ZJRK EOS. Very representative gas-oil relative permeability curves were used. The ability to match the slimtube tests with representative relative permeability curves gives added credibility to the EOS. Good matches were obtained for the oil recovery as a function of the volume of CO₂ injected for several pressures. Shown in Figure 26 are results for a pressure below the MMP (1,100 psia), a pressure near the MMP (1,212 psia), and a pressure above the MMP (3,000 psia). The simulated pressure for the 1,212 psia slimtube test was about 1,235 psia. Experimentally, at the 1,100 psia pressure, the injected CO₂ did not displace an equal volume of oil from the slimtube even at the start of the test; rather, a substantial portion of the CO₂ dissolved in the oil. The equation of state was able to match this behavior. The ability of the EOS to predict proper behavior below the MMP is important because the H-n-P tests will initially be operating below the MMP in the near-wellbore vicinity.

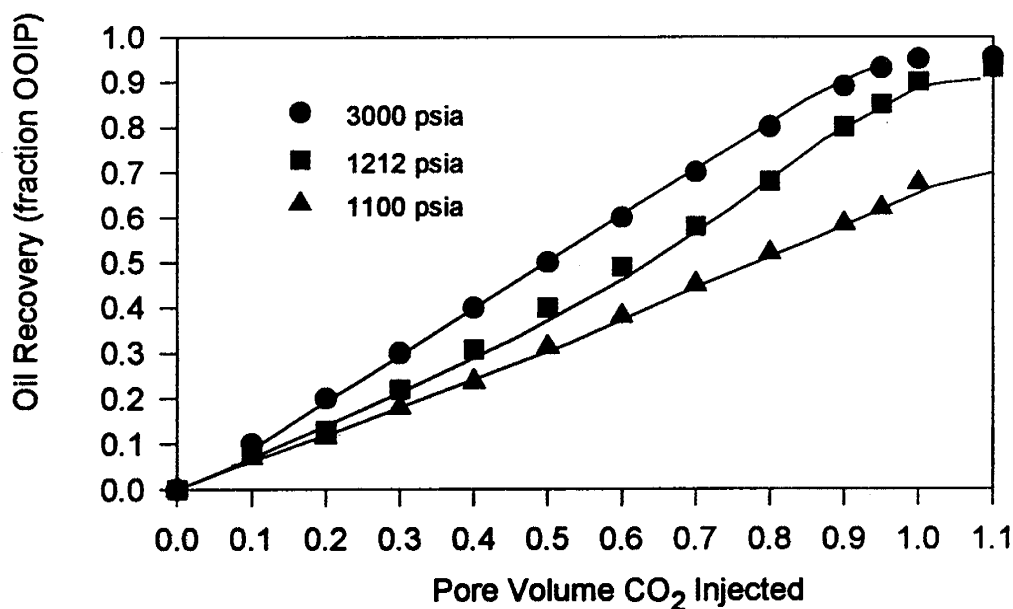


Figure 26: Comparison of laboratory slimtube data and simulations of oil recovery as a function of injected CO₂ volume for selected pressures. (Solid lines are simulations)

PARAMETRIC SIMULATIONS

With the EOS developed, a study of the various parameters effecting the technology will be undertaken with a compositional simulator. An investigation into the use of local grid refinement is underway.

A local grid refinement option in Western Atlas' VIP compositional simulator is available. This option allows for finer gridding in local regions within a coarser reservoir model. This will allow for smaller grids near a CO₂ H-n-P well while controlling computer run-time with larger grids in the surrounding reservoir. This option is a prerequisite to proper evaluation of the proposed technology.

A short investigation was done to evaluate the significance of grid size and various finite difference approximations on predicted oil recovery. A clear significance of nine-point versus five-point finite difference approximations was found when dealing with a coarser grid. Local grid refinement in this case did not appear to have a significant effect on oil recovery. A finer grid was made which resulted in similar recoveries for both the five-point and nine-point approximations. The conclusion of these initial exercises was that local grid refinement may not be necessary for a nine-point formulation. However, the benefits of local grid refinement to the analysis of near wellbore effects, such as pressure, which will dominate much of the field demonstrations has not yet been addressed.

Future work will involve the actual parametric simulations of the H-n-P process. A finely gridded radial model will be used so that accurate pressure profiles near the well bore can be determined. The parameters investigated will include both reservoir characteristics and operating strategies.

REFERENCES

- 1 ICF Resources Inc., "A Review of Shallow-Shelf Carbonate Reservoirs in the United States", U.S. DOE Contract DE-AC22-91BC14839, (August 1992).
- 2 Various speakers, DOE Pre-Proposal Conference, "Shallow Shelf Carbonates, Program Opportunity Notice, Class II Oil Program", presented October 22, 1992, Dallas, TX.
- 3 H. K. Haskin, R. B. Alston, "An Evaluation of CO₂ Huff 'n' Puff Field Tests in Texas", SPE Paper No. 15502, presented at SPE Annual Tech. Conf., New Orleans, LA, (10/5-8/86).
- 4 F. S. Palmer, R. W. Landry, S. Bou-Mikael, "Design and Implementation of Immiscible Carbon Dioxide Displacement Projects (CO₂ Huff-Puff) in South Louisiana", SPE Paper No. 15497 presented at SPE Annual Tech. Conf., New Orleans, LA, (10/5-8/86).
- 5 B.J. Miller, "Design and Results of a Shallow, Light Oilfield-Wide Application of CO₂ Huff 'n' Puff Process", SPE Paper No. 20268, Presented at the SPE/DOE Enhanced Oil Recovery Symposium in Tulsa, OK, (April 1990).
- 6 John T. Patton, Keith H. Coats, Ken Spence; "Carbon Dioxide Well Stimulation: Part 1 -- A Parametric Study", SPE Journal of Petroleum Technology, (August 1982).
- 7 John T. Patton, et al; "Carbon Dioxide Well Stimulation: Part 2 -- Design of Aminoil's North Bolsa Strip Project", SPE Journal of Petroleum Technology, (August 1982).
- 8 G.A. Thomas, T.G. Monger, "The Feasibility of Cyclic CO₂ Injection for Light-Oil Recovery", Paper No. 20208, presented at the SPE Enhanced Oil Recovery Symposium, Tulsa, OK, (4/22-25/90).
- 9 M. R. Simpson, "The CO₂ Huff 'n' Puff Process in a Bottomwater-Drive Reservoir", SPE Journal of Petroleum Technology, Paper No. 16720, (July 1988).
- 10 J. W. Amyx, D. M. Bass, & R. L. Whiting, "Petroleum Reservoir Engineering, Physical Properties," (1960).
- 11 H. C. Slider, "Worldwide Practical Petroleum Reservoir Engineering Methods," (1983).
- 12 J. T. Smith, "Petroleum Reservoir Engineering, Vol. I," (1980).
- 13 Vacuum Field Engineering Committee, "Vacuum Pool Report," Book I & II, 352 pages & exhibits, (1945)
- 14 D. M. Williams, "Vacuum Fd., Western Segment, Lea Co., NM, Feasibility of Waterflooding," (09-30-63).

- 15 Unknown Texaco Author(s), "Texaco Inc., Reservoir Study, Proposed Vacuum Grayburg San Andres Unit, Vacuum Field, Lea County, NM," (July 1972).
- 16 Unknou Texaco Author(s), "Reservoir & Waterflood Feasibility Study, Proposed Central Vacuum Unit, Lea Co., NM," (Aug., 1974).
- 17 Unknown Phillips Author(s), "A Unitized Water Injection Proposal for the East Vacuum Grayburg-San Andres Pool, Lea Co., NM," (May 1961).
- 18 Core Laboratories, Inc., "The Fundamentals of Core Analysis MOD II," (1981).
- 19 Widener, M. W. and Notz, P. K.: "CO₂ Swelling/Solubility Studies for Reservoir Fluids of the Central Vacuum Unit, Grayburg/San Andres Field, Lea County, New Mexico," Texaco EPTD Report 89-124, Houston (1989).
- 20 Hsu, J. C.: "Minimum Miscibility Pressure for CO₂ in Oil from Central Vacuum Unit, Vacuum Grayburg/San Andres Field, Lea County, New Mexico," Texaco EPTD Report 89-81, Houston (1989).

